Reaction of $[Et_4N]_2[Te\{Cr(CO)_5\}_n]$ ($n = 2, 3$) toward Electrophiles: Reactivity Comparison and Theoretical Calculations

Minghuey Shieh,* Li-Fang Ho, Pei-Chi Chen, Miao-Hsing Hsu, Hui-Lung Chen, Yu-Wen Guo, Yi-Wen Pan, and Yi-Chun Lin

Department of Chemistry, National Taiwan Normal University, Taipei 116, Taiwan, Republic of China

Received August 2, 2007

Reactions of $[Et_4N]_2[Te\{Cr(CO)_5\}_n]$ ($n = 2, 3$) with a series of organic and inorganic electrophiles have been systematically studied and compared. When $[Et_4N]_2[Te\{Cr(CO)_5\}_2]$ was protonated with ~1.0 equiv of HBF_4 in MeCN, the monohydrido Te−Cr complex $[Et_4N][HTe\{Cr(CO)_5\}_2]$ ($[Et_4N][\mathbf{1}]$) was obtained. However, similar protonation of $[Et_4N]_2[Te\{Cr(CO)_5\}_3]$ led to the formation of the decomposition product $[Et_4N]_2[Te_2\{Cr(CO)_5\}_4]$. While methylation of $[Et_4N]_2[Te\{Cr(CO)_5\}_2]$ with CF_3SO_3Me formed mono- and dimethylated products $[Et_4N][MeTe\{Cr(CO)_5\}_2]$ and $Me_2Te\{Cr(CO)_5\}_2$ (**2**) stepwise, a similar reaction with $[Et_4N]_2[Te\{Cr(CO)_5\}_3]$ produced the monomethylated product $[Et_4N][MeTe\{Cr(CO)_5\}_3]$ (**3**). Further, when $[Et_4N]_2[Te\{Cr(CO)_5\}_n]$ ($n = 2, 3$) was stirred in CH_2Cl_2 at 0 °C, the Cl-functionalized products $[Et_4N][ClH_2CTe\{Cr(CO)_5\}_n]$ ($n = 2$, $[Et_4N][\mathbf{4}]$; $n = 3$, $[Et_4N][\mathbf{5}]$) were produced, respectively. Similar reactions with CH_2Cl_2 at room temperature produced corresponding CH_2-bridged dimeric products $[Et_4N]_2[CH_2Te_2\{Cr(CO)_5\}_n]$ ($n = 4$; 6, $[Et_4N]_2[\mathbf{6}]$). If the bisbenzyl-containing reagent $ClH_2C(C_6H_4)_2CH_2Cl$ reacted with $[Et_4N]_2[Te\{Cr(CO)_5\}_n]$ ($n = 2, 3$), the corresponding $CH_2(C_6H_4)_2CH_2$-bridged dimeric complexes $[Et_4N]_2[H_2C(C_6H_4)_2CH_2Te_2\{Cr(CO)_5\}_n]$ ($n = 4$, $[Et_4N]_2[\mathbf{7}]$; $n = 6$, $[Et_4N]_2[\mathbf{8}]$) were produced. $[Et_4N]_2[Te\{Cr(CO)_5\}_n]$ ($n = 2, 3$) could further react with $HgCl_2$ in THF to give corresponding Hg-bridged products $[Et_4N]_2[HgTe_2\{Cr(CO)_5\}_n]$ ($n = 4$, $[Et_4N]_2[\mathbf{9}]$; $n = 6$, $[Et_4N]_2[\mathbf{10}]$). Complex **9** was found to transform to complex **10** upon its reaction with $HgCl_2$ in THF. Interestingly, the novel O_2-activation product $[Et_4N][OTe\{Cr(CO)_5\}_2]$ ($[Et_4N][\mathbf{11}]$) was observed when $[Et_4N]_2[Te\{Cr(CO)_5\}_2]$ was bubbled with O_2 in MeCN. Complexes **1**−**11** were fully characterized by elemental analysis, spectroscopic methods, and/or single-crystal X-ray analysis. The nature of $[Te\{Cr(CO)_5\}_n]^{2-}$ ($n = 2, 3$) and the resultant complexes were further investigated by molecular orbital calculations at the B3LYP level of the density functional theory.

Introduction

Soluble transition-metal sulfide complexes have been extensively studied because of their relevance to biological and industrial catalysts. In contrast, the chemistry of the analogues of tellurium, the heavier congener of sulfur, has been much less explored.[1] While the chemistry of iron-containing carbonyl telluride complexes has been well studied, the study of chromium-containing carbonyl tellurides remained relatively rare mainly due to a lack of practical synthetic methodologies.[1−3] For the Te−Cr−CO system, the structurally characterized examples were limited to some open structures such as $[Te_2\{Cr(CO)_5\}_4]^{2-}$,[4] $[Te_3\{Cr(CO)_5\}_4]^{2-}$,[4] $[Te_2\{Cr(CO)_5\}_2]^{2-}$,[5] and $[Te_3\{Cr(CO)_5\}]^{2-}$,[5] and only several ring complexes $[Te_4\{Cr(CO)_5\}_4]$,[6] $[Te_2\{Cr(CO)_4\}_2\{Cr(CO)_5\}_2]^{2-}$,[4] and $[Te_4Cr(CO)_4]^{2-}$ were reported.[7] Because of our interest in the chemistry of main group-transition metal carbonyl complexes,[8−10] two monotelluride-bridged dichromium and trichromium anionic species $[Te\{Cr(CO)_5\}_n]^{2-}$ ($n = 2, 3$) were successfully synthesized from the reaction of Te powder with $Cr(CO)_6$ in KOH/MeOH solutions.[10a] These two species can be isolated as $[Et_4N]^+$ salts and have been proven to be important intermediates for the

* To whom correspondence should be addressed. E-mail: mshieh@ntnu.edu.tw.

(1) (a) Roof, L. C.; Kolis, J. W. *Chem. Rev.* **1993**, *93*, 1037. (b) Gysling, H. J. *Coord. Chem. Rev.* **1982**, *42*, 133. (c) Sekar, P.; Ibers, J. A. *Inorg. Chem.* **2002**, *41*, 450 and references therein. (d) Shriver, D. F.; Kaesz, H. D.; Adams, R. D. *The Chemistry of Metal Cluster Complexes*; VCH Publishers: New York, 1990. (e) Whitmire, K. H. *Adv. Organomet. Chem.* **1997**, *42*, 1. (f) Mathur, P. *Adv. Organomet. Chem.* **1997**, *41*, 243. (g) Shieh, M. *J. Cluster Sci.* **1999**, *10*, 3.

(2) Goh, L. Y. *Coord. Chem. Rev.* **1999**, *185*−*186*, 257.

(3) Shieh, M.; Ho, L.-F.; Jang, L.-F.; Ueng, C.-H.; Peng, S.-M.; Liu, Y.-H. *Chem. Commun.* **2001**, 1014.

(4) Roof, L. C.; Pennington, W. T.; Kolis, J. W. *Inorg. Chem.* **1992**, *31*, 2056.

(5) Stauf, S.; Reisner, C.; Tremel, W. *Chem. Commun.* **1996**, 1749.

(6) Blacque, O.; Brunner, H.; Kubicki, M. M.; Nuber, B.; Stubenhoffer, B.; Wachter, J.; Wrackmeyer, B. *Angew. Chem., Int. Ed. Engl.* **1997**, *36*, 352.

(7) Flomer, W. A.; O'Neal, S. C.; Kolis, J. W.; Jeter, D.; Cordes, A. W. *Inorg. Chem.* **1988**, *27*, 969.

(8) (a) Shieh M.; Liou, Y.; Peng, S.-M.; Lee, G.-H. *Inorg. Chem.* **1993**, *32*, 2212. (b) Shieh, M.; Chen, P.-F.; Peng, S.-M.; Lee, G.-H. *Inorg. Chem.* **1993**, *32*, 3389. (c) Shieh, M.; Tsai, Y.-C. *Inorg. Chem.* **1994**, *33*, 2303. (d) Shieh, M.; Shieh, M.-H.; Tsai, Y.-C.; Ueng, C.-H. *Inorg. Chem.* **1995**, *34*, 5088. (e) Shieh, M.; Tang, T.-F.; Peng, S.-M.; Lee, G.-H. *Inorg. Chem.* **1995**, *34*, 2797. (f) Shieh, M.; Sheu, C.-m.; Ho, L.-F.; Cherng, J.-J.; Jang, L.-F.; Ueng, C.-H.; Peng, S.-M.; Lee, G.-H. *Inorg. Chem.* **1996**, *35*, 5504. (g) Cherng, J.-J.; Tsai, Y.-C.; Ueng, C.-H.; Lee, G.-H.; Peng, S.-M.; Shieh, M. *Organometallics* **1998**, *17*, 255. (h) Huang, K.-C.; Shieh, M.-H.; Jang, R.-J.; Peng, S.-M.; Lee, G.-H.; Shieh, M. *Organometallics* **1998**, *17*, 5202. (i) Shieh, M.; Chen, H.-S.; Chi, H.-H.; Ueng, C.-H. *Inorg. Chem.* **2000**, *39*, 5561. (j) Lai, Y.-W.; Cherng, J.-J.; Sheu, W.-S.; Lee, G.-A.; Shieh, M. *Organometallics* **2006**, *25*, 184. (k) Shieh, M.; Liou, Y.; Hsu, M.-H.; Chen, R.-T.; Yeh, S.-J.; Peng, S.-M.; Lee, G.-H. *Angew. Chem., Int. Ed.* **2002**, *41*, 2384.

(9) (a) Huang, K.-C.; Tsai, Y.-C.; Lee, G.-H.; Peng, S.-M.; Shieh, M. *Inorg. Chem.* **1997**, *36*, 4421. (b) Shieh, M.; Chen, H.-S.; Yang, H.-Y.; Ueng, C.-H. *Angew. Chem., Int. Ed.* **1999**, *38*, 1252. (c) Shieh, M.; Chen, H.-S.; Yang, H.-Y.; Lin, S.-F.; Ueng, C.-H. *Chem.-Eur. J.* **2001**, *7*, 3152. (d) Shieh, M.; Hsu, M.-H. *J. Cluster Sci.* **2004**, *15*, 91.

10.1021/om700789a CCC: $37.00
Publication on Web 11/01/2007

construction of many chromium carbonyl telluride complexes such as $[Te_2\{Cr(CO)_5\}_4]^{2-}$,[4] $[Te_3\{Cr(CO)_5\}_4]^{2-}$,[4] and $[Te_2\{Cr(CO)_4\}_2\{Cr(CO)_5\}_2]^{2-}$,[4] which were known to be obtained only by using Zintl ions as tellurido sources.[4]

Previous work revealed that metal or mixed-metal tellurido clusters are scarce.[11] Based on the lone pairs on the Te atoms of $[Et_4N]_2[Te\{Cr(CO)_5\}_n]$ ($n = 2$, 3) and their good solubility in organic solvents, these anionic complexes are potentially good candidates for further study of their interaction with either organic or inorganic electrophiles. Although the use of metal sulfides as synthons for such applications has been well documented, analogous reactions for metal tellurides have been limited.[1,11,12] Hence, the reactions of $[Te\{Cr(CO)_5\}_n]^{2-}$ ($n = 2$, 3) with electrophiles can definitely shed light on the basicity and nucleophilicity of tellurido ligands in transition metal complexes. In this study, we systematically described and compared the reactions of $[Et_4N]_2[Te\{Cr(CO)_5\}_n]$ ($n = 2$, 3) with a series of organic and inorganic electrophiles. The nature of these Te−Cr complexes and their formation are also elucidated by molecular orbital calculations at the B3LYP level of the density functional theory.

Results and Discussion

Reactions of $[Et_4N]_2[Te\{Cr(CO)_5\}_n]$ ($n = 2$, 3) with HBF_4 and CF_3SO_3Me. Because there are one or two lone pairs on the Te atom of $[Et_4N]_2[Te\{Cr(CO)_5\}_n]$ ($n = 3$, 2), the basicity of the Te atom was tested by the reactions with acidification and methylation agents. In a previous study, the direct acidification of Te−Cr carbonyl clusters was reported only in the case of the neutral complex $Te[(Cp^*)Cr(CO)_3]_2$, in which protonation was believed to occur at the Te atom.[13] However, there was no direct evidence reported for its existence at that time.

In this study, when $[Et_4N]_2[Te\{Cr(CO)_5\}_2]$ was acidified with ~1.0 equiv of HBF_4 in MeCN at −40 °C, the monohydrido complex $[Et_4N][HTe\{Cr(CO)_5\}_2]$ ($[Et_4N][\mathbf{1}]$) was obtained in a 65% yield. The infrared spectra of $[Et_4N][\mathbf{1}]$ showed the absorptions at 2046 w, 2031 m, 1932 s, and 1879 m cm^{-1}, which is characteristic of the terminal carbonyls and similar to those for $[Et_4N]_2[Te\{Cr(CO)_5\}_2]$,[10a] but shifted a bit to higher frequencies. Additionally, the ^1H NMR spectrum of $[Et_4N][\mathbf{1}]$ gave a signal at $\delta = -10.00$ for the H atom attached to the Te atom, and its formulation was further supported by elemental analysis. However, treatment of $[Et_4N]_2[Te\{Cr(CO)_5\}_3]$ with HBF_4 failed to yield the hydrido complex because of its lower basicity versus $[Et_4N]_2[Te\{Cr(CO)_5\}_2]$. This reaction, instead, led to the formation of the known complex $[Et_4N]_2[Te_2\{Cr(CO)_5\}_4]$,[4] which resulted from the dimerization of the decomposed fragment "$[Te\{Cr(CO)_5\}_2]$" due to weak Te−Cr bonds (Scheme 1).

Scheme 1

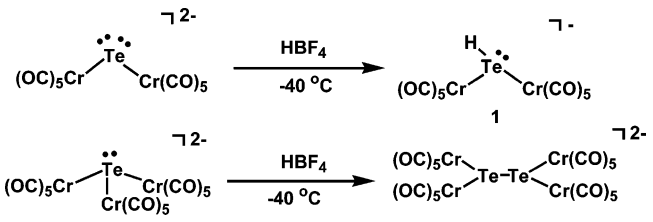

When $[Et_4N]_2[Te\{Cr(CO)_5\}_2]$ was treated with ~0.8 equiv of CF_3SO_3Me in MeCN at −40 °C, the Te-monomethylated product $[Et_4N][MeTe\{Cr(CO)_5\}_2]$[10a] was obtained in a 75% yield. Similarly, methylation of $[Me_4N]_2[Te\{Cr(CO)_5\}_3]$ with ~0.8 equiv of CF_3SO_3Me in MeCN produced the monomethylated product $[Me_4N][MeTe\{Cr(CO)_5\}_3]$ ($[Me_4N][\mathbf{3}]$) in a 90% yield. $[Et_4N][MeTe\{Cr(CO)_5\}_2]$ could be further methylated by the addition of ~1.0 equiv of CF_3SO_3Me to form the neutral dimethylated product $Me_2Te\{Cr(CO)_5\}_2$ (**2**) in good yields. Complex **2** could also be obtained directly from $[Et_4N]_2[Te\{Cr(CO)_5\}_2]$ with excess CF_3SO_3Me in an 85% yield (Scheme 2). Complex **2** was previously reported to be obtained from the reaction of $Cr(CO)_5THF$ with Me_2Te in THF; however, there was no crystal structure presented at that time.[14]

Complex **2** and $[Me_4N]_2[\mathbf{3}]$ were fully structurally characterized by single-crystal X-ray analysis, elemental analysis, and spectroscopic methods. X-ray analysis showed that complex **2** and anion **3** both displayed a tetrahedral geometry, in which the central tellurium atom for **2** was tetrahedrally coordinated by the two methyl groups and two $Cr(CO)_5$ fragments. The central tetrahedral tellurium atom for **3** was coordinated by the one methyl group and three $Cr(CO)_5$ fragments. The infrared spectra of **2** and **3** showed absorptions characteristic of the terminal carbonyls. The ^1H NMR spectrum of **2** gave one signal at $\delta = 2.45$ for the two methyl groups attached to the Te atom, and this value was close to that in MeTePh ($\delta = 2.1$),[15] but shifted downfield as compared to those in Me_2Te ($\delta = 1.84$)[14] and $[MeTe\{Cr(CO)_5\}_2]^-$ ($\delta = 1.7$).[10a] Further, the ^{13}C NMR spectrum of **2** showed one resonance at −0.82 for the two methyl groups. For the anion **3**, the methyl group gave the ^1H and ^{13}C NMR absorptions at $\delta = 2.07$ and $\delta = -15.92$, respectively. As compared to those ($\delta = 1.76$, −30.44) in $[MeTe\{Cr(CO)_5\}_2]^-$,[10a] these values for $[MeTe\{Cr(CO)_5\}_3]^-$ (**3**) shifted downfield due to the lack of a lone pair on the Te atom.

Reactions of $[Et_4N]_2[Te\{Cr(CO)_5\}_n]$ ($n = 2$, 3) with Organodihalides. Investigation of $[Et_4N]_2[Te\{Cr(CO)_5\}_n]$ ($n = 2$, 3) with organodihalides can provide some information regarding their ability to function as building blocks for further skeleton-expansion reactions. $[Et_4N]_2[Te\{Cr(CO)_5\}_2]$ was found to be unstable in CH_2Cl_2 and could react readily with CH_2Cl_2 at 0 °C to form the Cl-functionalized product $[Et_4N][ClCH_2Te\{Cr(CO)_5\}_2]$ ($[Et_4N][\mathbf{4}]$) in an 86% yield. Complex **4** could further act as an electrophile to react with $[Et_4N]_2[Te\{Cr(CO)_5\}_2]$ to give the known CH_2-bridged dimeric complex $[Et_4N]_2[H_2CTe_2\{Cr(CO)_5\}_4]$ (in a 58% yield), which could also be obtained directly from stirring of $[Et_4N]_2[Te\{Cr(CO)_5\}_2]$ in CH_2Cl_2 at room temperature[10a] (Scheme 3). Similarly, when $[Et_4N]_2[Te\{Cr(CO)_5\}_3]$ was treated with CH_2Cl_2 at 0 °C, the Cl-functionalized product $[Et_4N][ClCH_2Te\{Cr(CO)_5\}_3]$ ($[Et_4N][\mathbf{5}]$) was obtained in an 85% yield. Further stirring of $[Et_4N]_2[Te\{Cr(CO)_5\}_3]$ in CH_2Cl_2 at room temperature produced the

(10) (a) Shieh, M.; Ho, L.-F.; Guo, Y.-W.; Lin, S.-F.; Lin, Y.-C.; Peng, S.-M.; Liu, Y.-H. *Organometallics* **2003**, *22*, 5020. (b) Cherng, J.-J.; Lai, Y.-W.; Liu, Y.-H.; Peng, S.-M.; Ueng, C.-H.; Shieh, M. *Inorg. Chem.* **2001**, *40*, 1206. (c) Shieh, M.; Cherng, J.-J.; Lai, Y.-W.; Ueng, C.-H.; Peng, S.-M.; Liu, Y.-H. *Chem.-Eur. J.* **2002**, *8*, 4522. (d) Shieh, M.; Chung, R.-L.; Yu, C.-H.; Hsu, M.-H.; Ho, C.-H.; Peng, S.-M.; Liu, Y.-H. *Inorg. Chem.* **2003**, *42*, 5477. (e) Shieh, M.; Lin, S.-F.; Guo, Y.-W.; Hsu, M.-H.; Lai, Y.-W. *Organometallics* **2004**, *23*, 5182. (f) Hsu, M.-H.; Chen, R.-T.; Sheu, W.-S.; Shieh, M. *Inorg. Chem.* **2006**, *45*, 6740.

(11) Nakagawa, T.; Seino, H.; Nagao, S.; Mizobe, Y. *Angew. Chem., Int. Ed.* **2006**, *45*, 7758 and references therein.

(12) (a) Shieh, M.; Chen, P.-F.; Tsai, Y.-C.; Shieh, M.-H. *Inorg. Chem.* **1995**, *34*, 2251. (b) Shieh, M.; Shieh, M.-H. *Organometallics* **1994**, *13*, 920. (c) Shieh, M.; Chen, H.-S.; Lai, Y.-W. *Organometallics* **2004**, *23*, 4018.

(13) Herrmann, W. A.; Rohrmann, J. *J. Organomet. Chem.* **1984**, *273*, 221.

(14) Bremer, G.; Boese, R.; Keddo, M.; Kruck, T. *Z. Naturforsch.* **1986**, *41b*, 981.

(15) Hope, E. G.; Kemmitt, T.; Levason, W. *Organometallics* **1988**, *7*, 78.

Scheme 2

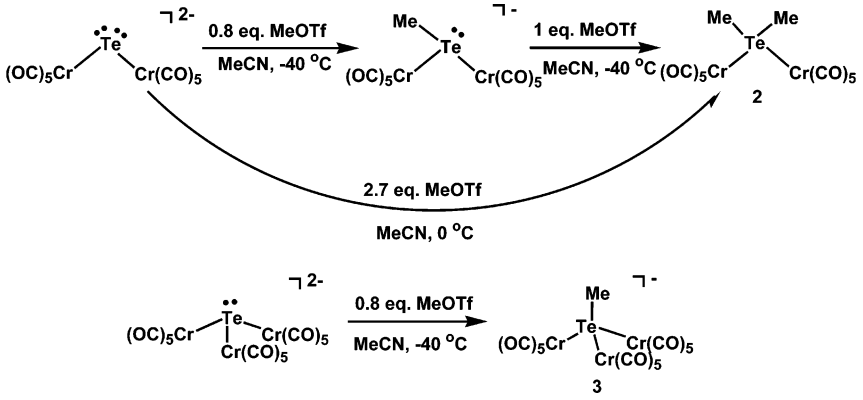

Scheme 3

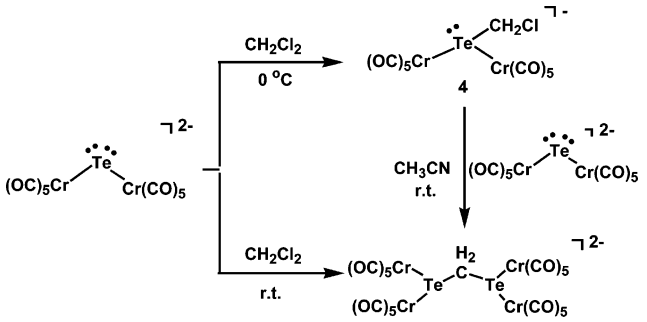

Scheme 4

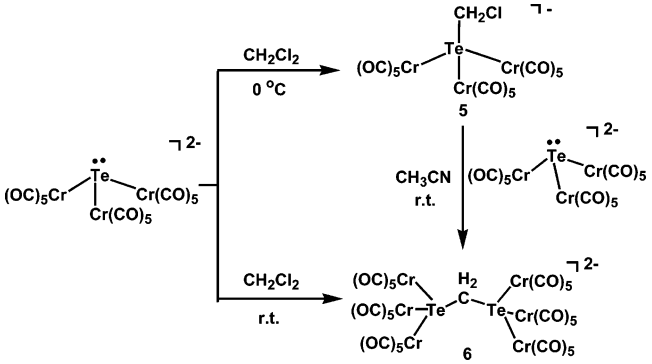

CH_2-bridged dimeric complex $[Et_4N]_2[H_2CTe_2\{Cr(CO)_5\}_6]$ ($[Et_4N]_2$[**6**]) in moderate yields. Like complex **4**, complex **5** is an effective electrophile for reacting with $[Et_4N]_2[Te\{Cr(CO)_5\}_3]$ to form $[Et_4N]_2$[**6**] (Scheme 4).

The new complexes **4**, **5**, and **6** were fully characterized by elemental analysis, spectroscopic methods, and/or single-crystal X-ray analysis. The X-ray analysis showed that anionic **4** possessed a tetrahedral geometry, in which the central tellurium atom was tetrahedrally coordinated by one CH_2Cl group and two $Cr(CO)_5$ fragments, leaving one lone pair uncoordinated. The ^{1}H and ^{13}C NMR spectra of the anion **4** gave signals at $\delta = 4.56$ and $\delta = -5.37$, respectively, for the CH_2Cl group attached to the Te atom. On the other hand, the X-ray analysis showed that anionic **5** displayed a tetrahedral geometry, in which the Te atom was tetrahedrally coordinated by one CH_2Cl group and three $Cr(CO)_5$ fragments. The ^{1}H and ^{13}C NMR spectra of **5** gave signals at $\delta = 4.55$ and $\delta = -6.41$, respectively, for the CH_2Cl group attached to the Te atom, which was close to those in complex **4**. This is indicative of the comparable effect of the lone pair and the $Cr(CO)_5$ fragment on the NMR absorptions. Furthermore, the infrared spectra of dianion **6** showed absorptions characteristic of the terminal carbonyls. The ^{1}H and ^{13}C NMR spectra of **6** gave signals at $\delta = 4.55$ and $\delta = -5.45$, respectively, for the bridging CH_2 group. As expected, these values compared favorably to those ($\delta = 4.53, -6.02$) observed for the CH_2-bridged dimeric complex $[Et_4N]_2[H_2CTe_2\{Cr(CO)_5\}_4]$.[10a]

Scheme 5

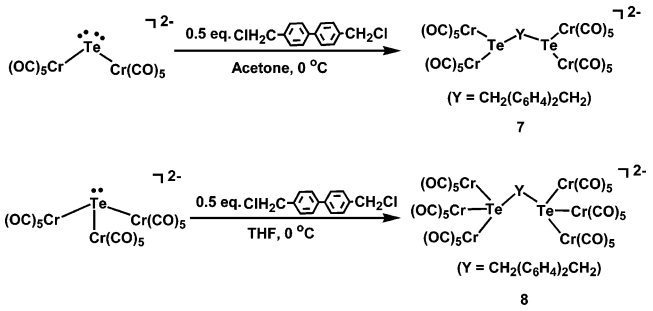

For comparison, reactions of $[Et_4N]_2[Te\{Cr(CO)_5\}_n]$ ($n = 2$, 3) with bisbenzyl-containing dichloride-$ClH_2C(C_6H_4)_2CH_2Cl$ were further investigated. The corresponding bisbenzyl-bridged complexes $[Et_4N]_2[H_2C(C_6H_4)_2CH_2Te_2\{Cr(CO)_5\}_n]$ ($n = 4$, $[Et_4N]_2$[**7**]; $n = 6$, $[Et_4N]_2$[**8**]) were obtained in 81% and 21% yields, respectively (Scheme 5). $[Et_4N]_2[Te\{Cr(CO)_5\}_n]$ ($n = 2$, 3) are considered to undergo the double nucleophilic attack onto the bisbenzyl-containing agent $ClH_2C(C_6H_4)_2CH_2Cl$ to form complexes **7** and **8**. These complexes were fully structurally characterized by X-ray analysis and spectroscopic methods. On the basis of the X-ray analysis, complex **7** had two molecules of $[Te\{Cr(CO)_5\}_2]^{2-}$ connected by the $H_2C(C_6H_4)_2CH_2^{2+}$ moiety, and complex **8** had two molecules of $[Te\{Cr(CO)_5\}_3]^{2-}$ linked by the $H_2C(C_6H_4)_2CH_2^{2+}$ moiety. The ^{1}H and ^{13}C NMR spectra of **7** gave signals at $\delta = 3.97$ and $\delta = -1.28$, respectively, for the bridging CH_2 segments, while those of **8** showed absorptions at $\delta = 3.98$ and $\delta = -0.98$, respectively. Again, these absorptions reflect the similar effect of a lone pair versus the $Cr(CO)_5$ fragment.

Reactions of $[Et_4N]_2[Te\{Cr(CO)_5\}_n]$ ($n = 2$, 3) with $HgCl_2$ and O_2. In addition to organic reagents, reactions of $[Et_4N]_2[Te\{Cr(CO)_5\}_n]$ ($n = 2$, 3) with mercury salts or O_2 were studied for comparison. Like organic dihalides, the reactions of $[Et_4N]_2[Te\{Cr(CO)_5\}_n]$ ($n = 2$, 3) with ~0.5 equiv of $HgCl_2$ in MeCN led to the formation of the Hg-bridged dimeric complexes $[Et_4N]_2[HgTe_2\{Cr(CO)_5\}_n]$ ($n = 4$, $[Et_4N]_2$[**9**]; $n = 6$, $[Et_4N]_2$[**10**]), respectively (Scheme 6). X-ray analysis showed that the Hg-bridged complexes **9** and **10** were structurally analogous to the organo-bridged complexes **7** and **8**, respectively. Further, complex **9** could transform to complex **10** upon treatment with ~0.5 equiv of $HgCl_2$ in MeCN, in which $HgCl_2$ acted as an oxidizing agent to cause the bond breakage and reformation of

Scheme 6

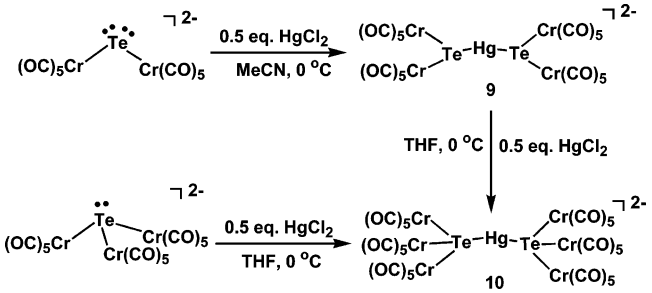

Scheme 7

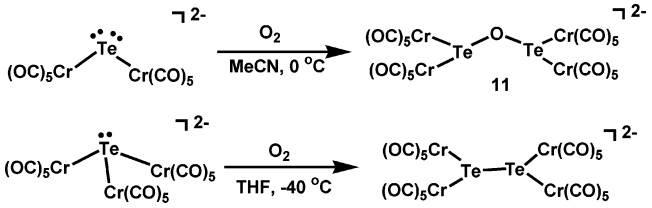

9 to give **10**. This was mainly due to weak Te−Cr bonds. Clusters **9** and **10** represent rare examples of mixed-metal telluride complexes, and further study on their cluster expansion and physical properties is under investigation.

Moreover, it was found that $[Et_4N]_2[Te\{Cr(CO)_5\}_n]$ ($n = 2$, 3) showed different reactivity toward the oxygen molecule. $[Et_4N]_2[Te\{Cr(CO)_5\}_2]$ could readily react with O_2 in MeCN to give the O-bridged complex $[Et_4N][OTe\{Cr(CO)_5\}_2]$ ([Et_4N]-[**11**]) in an almost quantitative yield, while the reaction with $[Et_4N]_2[Te\{Cr(CO)_5\}_3]$ only formed the oxidized known complex[4] $[Te_2\{Cr(CO)_5\}_4]^{2-}$ without observation of the analogous O-bridged product (Scheme 7). The activation of O_2 by $[Et_4N]_2$-$[Te\{Cr(CO)_5\}_2]$ is surprising as it is rare in the literature. The detailed mechanism is not clear at this moment but should be related to the low coordination and high reactivity of $[Te\{Cr(CO)_5\}_2]^{2-}$. It is noted that the Te−O bond of complex **11** was relatively weak, which was substantiated by the ease of elimination of the $Te\{Cr(CO)_5\}_2$ fragment of **11** in the ESI-MS study.

X-ray Structural Comparison of 2, $[Me_4N]$[3], $[Et_4N]$[4], [PPN][5], $[Et_4N]_2$[7], $[Me_4N]_2$[8], $[Et_4N]_2$[9], $[Et_4N]_2$[10], and $[Et_4N]_2$[11]. Complex **2** and anionic complexes **3**, **4**, **5**, **7**, **8**, **9**, **10**, and **11** can be viewed to have Te-centered chromium carbonyl-coordinated open structures. Complexes **2**, **4**, **7**, **9**, and **11** are considered to possess the $Te\{Cr(CO)_5\}_2$-based geometry, in which the Te atom is tetrahedrally bonded to two $Cr(CO)_5$ fragments and one or two ligands. While **2** consists of a Te-$\{Cr(CO)_5\}_2$ core with two methyl groups as ligands (Figure 1), **4** displays a $Te\{Cr(CO)_5\}_2$ core coordinated with one CH_2Cl group and with one uncoordinated lone pair (Figure 3). Besides, **7**, **9**, and **11** are isostructural and each have two $Te\{Cr(CO)_5\}_2$ units that are bridged by a $CH_2(C_6H_4)_2CH_2$ fragment, a Hg atom, or an O atom, respectively (Figures 5, 7, and 9). On the other hand, complexes **3**, **5**, **8**, and **10** are considered to have the Te-$\{Cr(CO)_5\}_3$-based structure, in which the Te atom is tetrahedrally bonded to three $Cr(CO)_5$ fragments and one coordinated ligand. While isostructural complexes **3** and **5** each have a Te-$\{Cr(CO)_5\}_3$ core externally bonded with a Me group or with a CH_2Cl group (Figures 2 and 4), isostructural complexes **8** and **10** each have two $Te\{Cr(CO)_5\}_3$ units that are bridged by either a $CH_2(C_6H_4)_2CH_2$ or a Hg atom (Figures 6 and 8).

For comparison, the selected bond distances and bond angles of the new Te−Cr complexes and related complexes are listed in Table 1. As shown in Table 1, the average Te−Cr distances

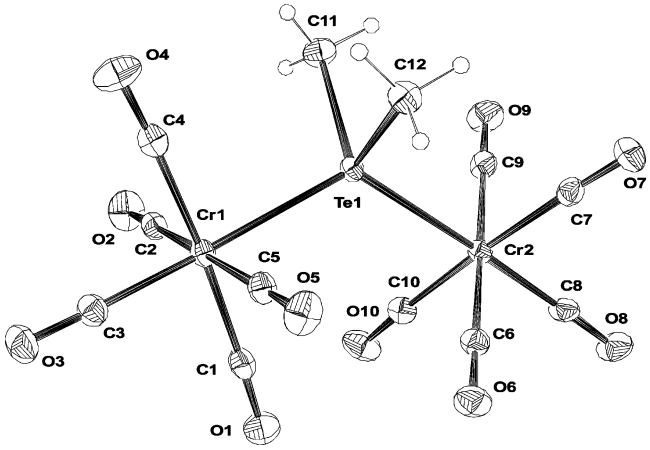

Figure 1. ORTEP diagram showing the structure and atom labeling for **2**.

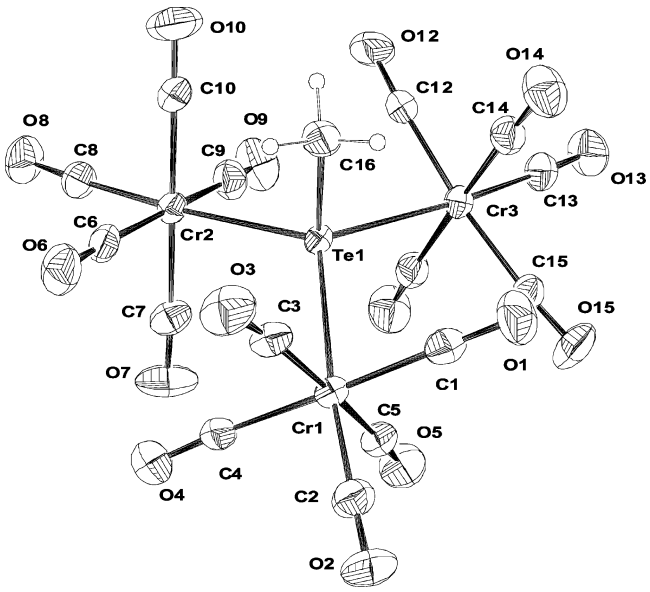

Figure 2. ORTEP diagram showing the structure and atom labeling for anion **3**.

in the new Te−Cr complexes are basically close to those reported in the other related polytelluride complexes such as $[Te_2\{Cr(CO)_5\}_4]^{2-}$ (2.749 Å),[4] $[Te_3\{Cr(CO)_5\}_4]^{2-}$ (2.763 Å),[4] $[Te_2\{Cr(CO)_5\}_2]^{2-}$ (2.739 Å),[5] and $[Te_3\{Cr(CO)_5\}]^{2-}$ (2.754 Å).[5] It is noted, however, that the average Te−Cr bond distance of **4** (2.720 Å) is the same as that of **5** (2.720 Å), indicative of little steric effect of the $Cr(CO)_5$ groups on the Te−Cr bond. A similar situation is also observed in the cases of **7** versus **8** and **9** versus **10**. The average Te−Cr bonds in **3**−**5** are only a bit shorter than those in **7**−**10**, reflecting the smaller steric effect of mono-$TeCr_n$- versus di-$TeCr_n$-based ($n = 2$, 3) structures. In addition, the average Te−Cr bonds for anionic Te−Cr complexes are significantly longer than that of the neutral complex **2** due to the effect of the negative charge.

The Cr−Te−Cr angles about the tellurium atom in **2**, **3**, **4**, **5**, **7**, **8**, **9**, **10**, and **11** range from 112.88° to 122.36°, which somewhat deviated from the regular tetrahedral angle. In general, the average Cr−Te−Cr angles for the $TeCr_2$-based complexes are a bit larger than those of their corresponding $TeCr_3$-based complexes due to the steric effect of the $Cr(CO)_5$ moiety. Further, the Cr−Te−Cr angle in **2** is the largest among the $TeCr_2$-based complexes due to the small steric hindrance of two methyl groups, while that of **3** is the largest among the $TeCr_3$-based complexes due to the smallest steric hindrance of one

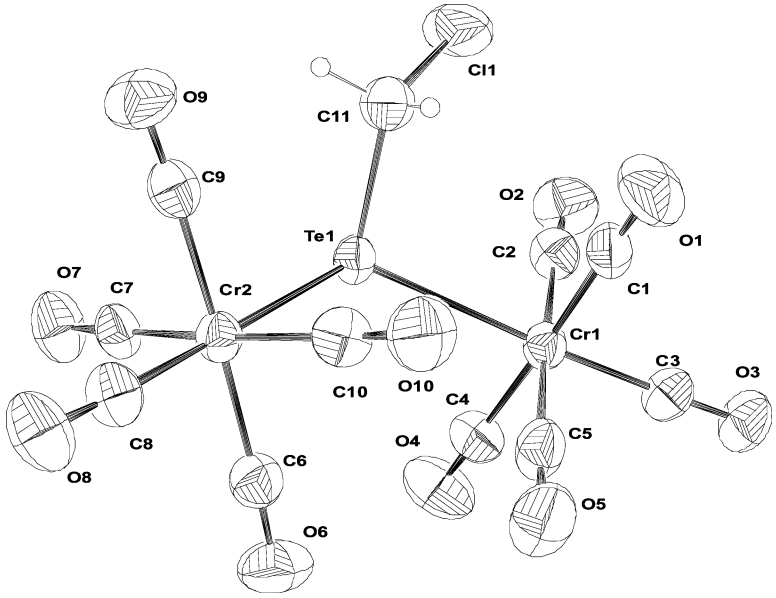

Figure 3. ORTEP diagram showing the structure and atom labeling for anion **4**.

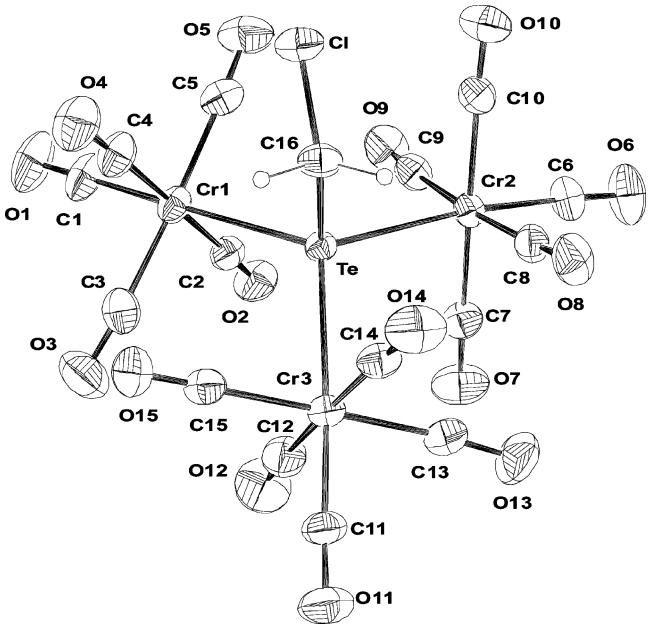

Figure 4. ORTEP diagram showing the structure and atom labeling for anion **5**.

methyl group versus other coordinated ligands. Additionally, the Te−O−Te bond angle of **11** is 108.2(3)°, indicative of the tetrahedral geometry around the O center, which is significantly larger than the Te−Te−Te angle (98.4(1)°) in the related complex[4] $[Te_3\{Cr(CO)_5\}_4]^{2-}$. This is attributed to the diminished s-character of the central Te atom caused by the larger size of Te versus O. The values in these two chalcogen-bridged complexes are smaller than the Te−C−Te angle (115.2(2)°) in the CH_2-bridged complex $[H_2CTe_2\{Cr(CO)_5\}_4]^{2-}$,[10a] due to the effect of the lone pairs of the chalcogen atom. Finally, the Te−C bonds in complexes **2**−**5**, **7**, and **8** are within the range of 2.135−2.22 Å, which is normal.

DFT Computation. To further portray the electronic structures of the $[Te\{Cr(CO)_5\}_n]^{2-}$ (n = 2, 3) and their relevant reaction phenomena, we employed a hybrid density functional (B3LYP[16,17]) with a modest basis set LanL2DZ for each complex. The molecular geometries are taken from single-crystal X-ray diffraction data. To examine scenarios of the framework for $[Te\{Cr(CO)_5\}_n]^{2-}$ (n = 2, 3) and their related products, we looked at their frontier molecular orbitals and the main orbital coefficients. The frontier molecular orbitals of $[Te\{Cr(CO)_5\}_n]^{2-}$ (n = 2, 3) and related products are shown in Figure 10, and the orbital compositions, which are expressed in terms of the contribution, are listed in Table 2. As shown in Figure 10, the HOMOs of complexes $[Te\{Cr(CO)_5\}_n]^{2-}$ (n = 2, 3) have a slightly antibonding interaction between the p orbital of the Te atom and d orbitals of the Cr atom, in which the significant contribution is from the p orbital (48% and 34%, respectively) of the central Te atom (see Table 2). It is interesting to note that when the consecutive methylation takes place on both $[Te\{Cr(CO)_5\}_n]^{2-}$ (n = 2, 3) (which formed new complexes **2** and **3**), a substantial alteration in the orbital coefficients of the central Te atoms was observed. Our calculated results indicate that the contribution from the p orbital of the HOMO of the $TeCr_2$-based complexes is (in decreasing order) $[Te\{Cr(CO)_5\}_2]^{2-}$ > $[MeTe\{Cr(CO)_5\}_2]^-$ > **2**, and $[Te\{Cr(CO)_5\}_3]^{2-}$ > **3** is found for the $TeCr_3$-based complexes (see Table 2). Therefore, the incoming electrophilic MeOTf could interact with the lone pair of the Te atom (prevailing contribution from the p orbital) of $[Te\{Cr(CO)_5\}_n]^{2-}$ (n = 2, 3), which would result in the decreasing contribution of the p orbital of the Te atom of their products. A similar explanation also could account for the reactions of $[Te\{Cr(CO)_5\}_n]^{2-}$ (n = 2, 3) with methylene chloride (CH_2Cl_2), in which the newly formed CH_2Cl-functionalized products **4** and **5** have smaller p orbital coefficients on the HOMOs than those of the initial reactants, $[Te\{Cr(CO)_5\}_n]^{2-}$ (n = 2, 3), respectively.

To understand the bonding nature of each complex, we also calculated the Wiberg bond index[18] and natural population analyses (NPA)[19] for complexes $[Te\{Cr(CO)_5\}_2]^{2-}$, $[MeTe\{Cr(CO)_5\}_2]^-$, **2**, $[Te\{Cr(CO)_5\}_3]^{2-}$, and **3**, which are listed in Table 3. Their corresponding structures are also illustrated in the lower part of this table. The analysis revealed that the Te

(16) (a) Becke, A. D. *J. Chem. Phys.* **1993**, *98*, 5648. (b) Becke, A. D. *J. Chem. Phys.* **1992**, *96*, 2155. (c) Becke, A. D. *J. Chem. Phys.* **1992**, *97*, 9173.
(17) Lee, C.; Yang, W.; Parr, R. G. *Phys. Rev.* **1988**, *B37*, 785.
(18) Wiberg, K. B. *Tetrahedron* **1968**, *24*, 1083.
(19) (a) Reed, A. E.; Weinhold, F. *J. Chem. Phys.* **1983**, *78*, 4066. (b) Reed, A. E.; Weinstock, R. B.; Weinhold, F. *J. Chem. Phys.* **1985**, *83*, 735.

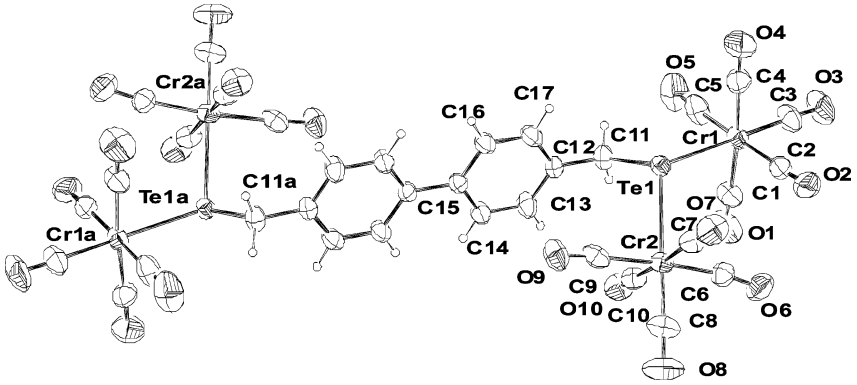

Figure 5. ORTEP diagram showing the structure and atom labeling for anion **7**.

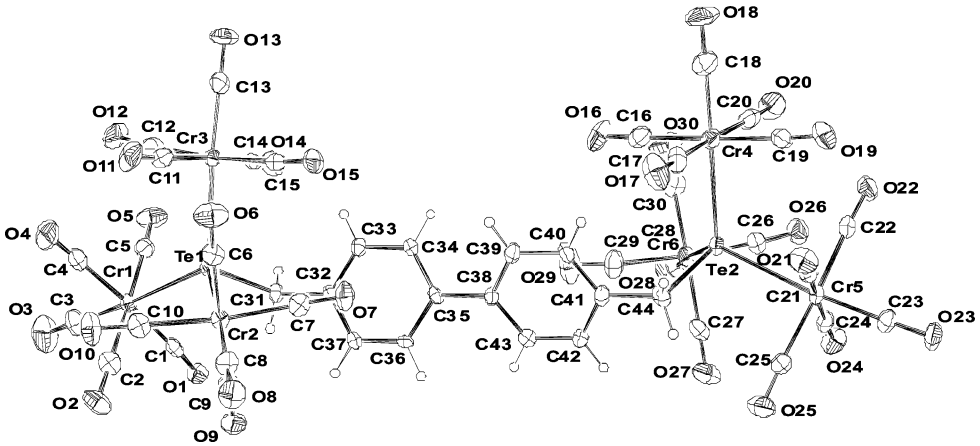

Figure 6. ORTEP diagram showing the structure and atom labeling for dianion **8**.

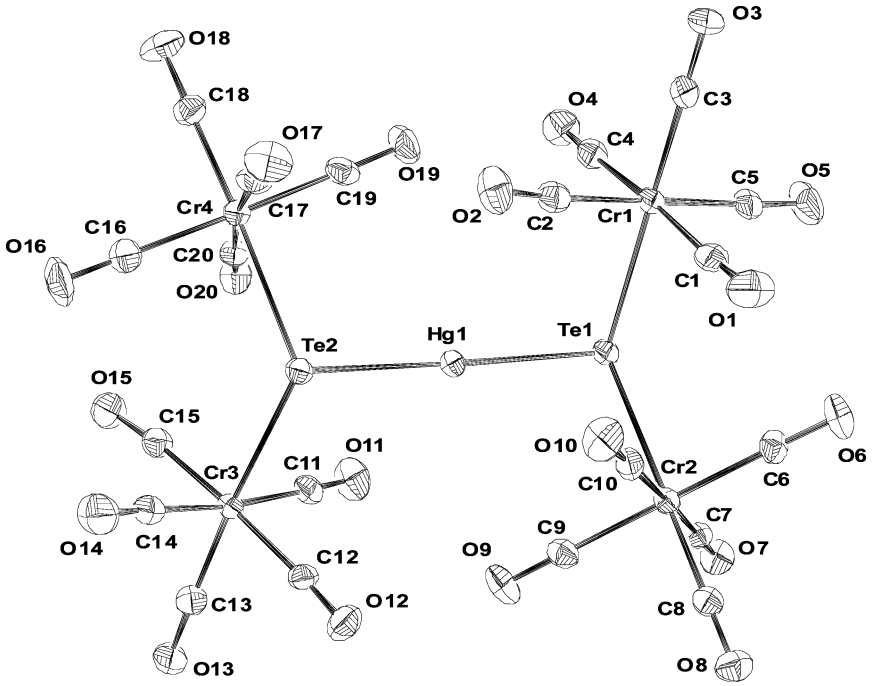

Figure 7. ORTEP diagram showing the structure and atom labeling for dianion **9**.

atom in $[Te\{Cr(CO)_5\}_2]^{2-}$, $[MeTe\{Cr(CO)_5\}_2]^-$, **2**, $[Te\{Cr(CO)_5\}_3]^{2-}$, and **3** each carried −0.39, +0.40, +1.17, −0.04, and +0.68 |e|, while the average charges of the Cr atom in those complexes were −1.36, −1.36, −1.43, −1.34, and −1.39 |e|. This indicated the inter-site coulomb attraction between Te−Cr bond on the $[Te\{Cr(CO)_5\}_n]^{2-}$ (n = 2, 3), and their relevant methylation derivatives occurred in the order of **2** > $[MeTe\{Cr(CO)_5\}_2]^-$ > $[Te\{Cr(CO)_5\}_2]^{2-}$, and **3** > $[Te\{Cr(CO)_5\}_3]^{2-}$, respectively. In addition, the calculated Wiberg bond indices (also called bond orders) of the aforementioned species also reflected the same tendency, in which more methylation occurred on both complexes $[Te\{Cr(CO)_5\}_n]^{2-}$ (n = 2, 3), and the larger mean Wiberg bond indices between Te and Cr atoms (Te−Cr bond) would be obtained (see Table 3).

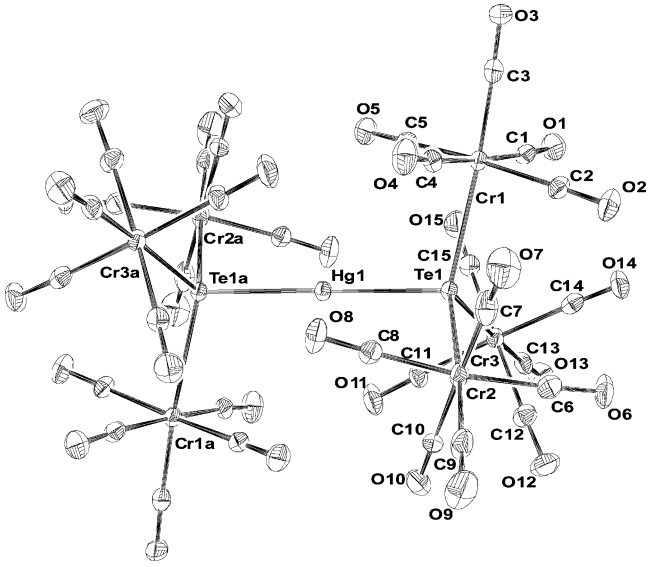

Figure 8. ORTEP diagram showing the structure and atom labeling for dianion **10**.

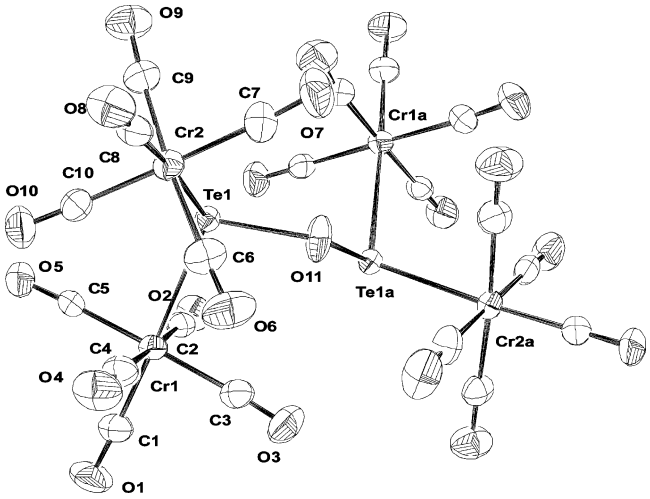

Figure 9. ORTEP diagram showing the structure and atom labeling for dianion **11**.

Furthermore, the Wiberg bond index and natural population analyses as well as the corresponding structures for the X-bridged Te−X−Te complexes (X = Hg, O, and CH_2) are displayed in Table 4. The frontier molecular orbitals are depicted in Figure 11, and orbital compositions are listed in Table 5. It is found that the HOMO of complex **9** in the central segment consists of small d orbitals (2%) of the Hg atom mixed with p orbitals (24%) of the Te atom. However, in the case of the counterpart of complex **10**, the bonding character of the HOMO in the central segment is derived mainly from the Hg (slight p orbitals, 3%) and Te (p orbitals, 12%) atomic orbitals (see Figure 11 and Table 4). Moreover, in regard to two isoelectronic analogues, **11** and $[H_2CTe_2\{Cr(CO)_5\}_4]^{2-}$, the calculations show that the bond index between Te−O (0.72) for complex **11** is smaller than that between Te−C (0.90) for $[H_2CTe_2\{Cr(CO)_5\}_4]^{2-}$. The computed results could not be clarified by means of the natural charge because the ionic-interaction difference between Te−O and Te−C was insignificant (see Table 4). As shown in Figure 11, the pictorial description of the HOMO in the Te−O−Te segment had an apparent antibonding interaction between the O atom (p orbital, 10%) and the Te atom (p orbital, 24%, mixed with some degree of s-character, 4%). This antibonding phenomenon is absent in the Te−C−Te counterpart, indicative of the more significant repulsion in the Te−O bond than in the Te−C bond. This explains why the average bond index calculated for Te−O is smaller than that calculated for Te−C (see Table 4).

Summary

The reactions of the monotelluride-bridged di- and trichromium carbonyl anions $[Et_4N]_2[Te\{Cr(CO)_5\}_n]$ ($n = 2, 3$) with a series of electrophiles were systematically studied. The tellurium atom of $[Et_4N]_2[Te\{Cr(CO)_5\}_n]$ ($n = 2, 3$) showed good affinity toward electrophiles in which the $TeCr_2$- and $TeCr_3$-based organo- or metal-incorporated monomeric or dimeric complexes were obtained. The nature of $[Et_4N]_2[Te\{Cr(CO)_5\}_n]$ ($n = 2, 3$) and their resultant products were also compared and elucidated by DFT calculations. This study provides a wide range of $TeCr_2$- and $TeCr_3$-based complexes for further investigation through practical and theoretical applications.

Experimental Section

All reactions were performed under an atmosphere of pure nitrogen using standard Schlenk techniques.[20] Solvents were purified, dried, and distilled under nitrogen prior to use. $Cr(CO)_6$ (Strem), Te powder (Strem), CF_3SO_3Me (Aldrich), HBF_4 (Strem), $HgCl_2$ (Shimakyu's), $ClH_2C(C_6H_4)_2CH_2Cl$ (Aldrich), and KOH (Showa) were used as received. Infrared spectra were recorded on a Perkin-Elmer Paragon 500 IR spectrometer as solutions in CaF_2 cells. The ^1H and ^{13}C NMR spectra were obtained on a JEOL 400 instrument and Bruker AV 400 at 399.78 and 100.53 MHz, respectively. EI mass spectra were taken on a Finningan TSQ 700 GC/LC/MS mass spectrometer. Elemental analyses for C, H, and N were performed on a Perkin-Elmer 2400 analyzer at the NSC Regional Instrumental Center at National Taiwan University, Taipei, Taiwan. $[Et_4N]_2[Te\{Cr(CO)_5\}_n]$ ($n = 2, 3$) was prepared according to the published procedures.[10a]

Reaction of $[Et_4N]_2[Te\{Cr(CO)_5\}_2]$ with HBF_4 (∼1:1.1) in MeCN. HBF_4 (0.22 mL, 1.70 mmol) was added to a MeCN solution (30 mL) of $[Et_4N]_2[Te\{Cr(CO)_5\}_2]$ (1.16 g, 1.50 mmol) at −40 °C. The green solution became yellowish-brown instantly. After being stirred for 60 min, the solution was filtered, and the solvent was evaporated under vacuum. The residue was washed with hexanes/Et_2O several times and extracted with THF to give a yellowish-brown sample of $[Et_4N][HTe\{Cr(CO)_5\}_2]$ ($[Et_4N][\mathbf{1}]$) (0.63 g, 0.98 mmol) (65% based on $[Et_4N]_2[Te\{Cr(CO)_5\}_2]$). IR ($\nu_{CO}$, MeCN): 2046 w, 2031 m, 1932 s, 1879 m cm^{-1}. Anal. Calcd for $[Et_4N][\mathbf{1}]$: C, 33.63; H, 3.29; N, 2.18. Found: C, 33.51; H, 2.96; N, 2.15. ^1H NMR (400 MHz, DMSO-d_6, 300 K, ppm): δ −10.00 (s, H) (chemical shifts not given for $[Et_4N]^+$).

Reaction of $[Et_4N]_2[Te\{Cr(CO)_5\}_3]$ with HBF_4 (∼1:0.5) in THF. HBF_4 (0.023 mL, 0.18 mmol) was added to a THF solution (30 mL) of $[Et_4N]_2[Te\{Cr(CO)_5\}_3]$ (0.41 g, 0.43 mmol) at −40 °C. The olive green solution became yellowish-brown instantly. After being stirred for 60 min, the solution was filtered, and the solvent was evaporated under vacuum. The residue was washed several times with Et_2O and extracted with THF to give a sample of $[Et_4N]_2[Te_2\{Cr(CO)_5\}_4]$[4] (0.08 g, 0.06 mmol) (27% based on $[Et_4N]_2[Te\{Cr(CO)_5\}_3]$). IR ($\nu_{CO}$, THF): 2058 w, 2038 m, 2031 s, 1965 w, 1929 vs, 1907 w, 1873 s cm^{-1}.

Reaction of $[Et_4N]_2[Te\{Cr(CO)_5\}_2]$ with CF_3SO_3Me (∼1:0.8) in MeCN. CF_3SO_3Me (0.12 mL, 1.10 mmol) was added to a MeCN solution (30 mL) of $[Et_4N]_2[Te\{Cr(CO)_5\}_2]$ (1.10 g, 1.42 mmol) at −40 °C. The green solution became yellowish-brown instantly.

(20) Shriver, D. F.; Drezdon, M. A. *The Manipulation of Air-Sensitive Compounds*; Wiley-VCH Publishers: New York, 1986.

Table 1. Average Bond Distance (Å) and Bond Angles (deg) for 2, $[Me_4N]$[3], $[Et_4N]$[4], [PPN][5], $[Et_4N]_2$[7], $[Me_4N]_2$[8], $[Et_4N]_2$[9], $[Et_4N]_2$[10], and $[Et_4N]_2$[11]

complex	Te−Cr, Å	Cr−Te−Cr, deg	Te−C, Å	ref
$Me_2Te\{Cr(CO)_5\}_2$ (**2**)	2.6434	122.36(3)	2.135	*a*
$[Me_4N][MeTe\{Cr(CO)_5\}_3]$ ($[Me_4N]_2$[**3**])	2.725	115.86	2.154(7)	*a*
$[Et_4N][ClCH_2CTe\{Cr(CO)_5\}_2]$ ($[Et_4N]$[**4**])	2.720	118.27(4)	2.140(8)	*a*
$[PPN][ClCH_2Te\{Cr(CO)_5\}_3]$ ($[Et_4N]$[**5**])	2.720	115.59	2.181(5)	*a*
$[Et_4N]_2[H_2C(C_6H_4)_2CH_2Te_2\{Cr(CO)_5\}_4]$ ($[Et_4N]_2$[**7**])	2.726	114.19	2.17	*a*
$[Me_4N]_2[H_2C(C_6H_4)_2CH_2Te_2\{Cr(CO)_5\}_6]$ ($[Me_4N]_2$[**8**])	2.739	113.90	2.22	*a*
$[Et_4N]_2[HgTe_2\{Cr(CO)_5\}_4]$ ($[Et_4N]_2$[**9**])	2.751	116.30		*a*
$[Et_4N]_2[HgTe_2\{Cr(CO)_5\}_6]$ ($[Et_4N]_2$[**10**])	2.732	115.04		*a*
$[Et_4N]_2[OTe_2\{Cr(CO)_5\}_4]$ ($[Et_4N]_2$[**11**])	2.737	112.88		*a*
$[Et_4N]_2[CH_2Te_2\{Cr(CO)_5\}_4]$	2.747	112.83	2.163(2)	10a
$[PPh_4]_2[Te_2\{Cr(CO)_5\}_4]$	2.749	116.90		4
$[PPh_4]_2[Te_3\{Cr(CO)_5\}_4]$	2.763	113.10		4
$[K(2,2,2\text{-crypt})]_2[Te_2\{Cr(CO)_5\}_2]$[b]	2.739			5
$[K(2,2,2\text{-crypt})]_2[Te_3\{Cr(CO)_5\}]$	2.754(5)			5
$[PPh_4]_2[Te_2\{Cr(CO)_4\}_2\{Cr(CO)_5\}_2]$	2.781 (out of plane) 2.692 (in plane)			4
$[Te_4\{Cr(CO)_5\}_4]$	2.587			6
$[PPh_4]_2[Te_4Cr(CO)_4]$	2.726			7

[a] This work. [b] 2,2,2-crypt = (4,7,13,16,21,24-hexaoxa-1,10-diazabicyclo[8.8.8]hexacosane).

Table 2. Calculated Percentage Contribution Ratios of the Te and Cr Atoms to Selected Frontier Molecular Orbitals of $[Te\{Cr(CO)_5\}_n]^{2-}$ (n = 2, 3) and Their Related Complexes

complexes	atoms	
	Te	Cr
$[Te\{Cr(CO)_5\}_2]^{2-}$ (HOMO)	48% p	10% d
$[Te\{Cr(CO)_5\}_2]^{2-}$ (LUMO)	14% s + 15% p	3% p + 4% d
$[MeTe\{Cr(CO)_5\}_2]^-$ (HOMO)	2% s + 16% p	21% d
$[MeTe\{Cr(CO)_5\}_2]^-$ (LUMO)	23% s + 13% p	11% p + 8% d
2 (HOMO)	6% s	2% p + 27% d
2 (LUMO)	20% s + 8% p	23% s + 8% p
$[Te\{Cr(CO)_5\}_3]^{2-}$ (HOMO)	2% s + 34% p	17% d
$[Te\{Cr(CO)_5\}_3]^{2-}$ (LUMO)	20% s + 8% p	7% p + 6% d
3 (HOMO)	4% p	2% s + 9% p + 38% d
3 (LUMO)	35% s	13% p + 8% d
4 (HOMO)	2% s + 24% p	25% d
4 (LUMO)	24% s + 11% p	11% p + 4% d
5 (HOMO)	2% s + 3% p	3% s + 8% p + 38% d
5 (LUMO)	36% s	15% p + 5% d

After being stirred for 1 h, the solution was filtered, and the solvent was evaporated under vacuum. The residue was washed several times with Et_2O and extracted with THF to give a yellowish-orange sample of $[Et_4N][MeTe\{Cr(CO)_5\}_2]$[10a] (0.54 g, 0.82 mmol) (75% based on CF_3SO_3Me). IR (ν_{CO}, THF): 2051 w, 2030 s, 1962 w, 1932 vs, 1906 m, 1890 s cm^{-1}.

Reaction of $[Et_4N]_2[Te\{Cr(CO)_5\}_2]$ with CF_3SO_3Me (~1:2.7) in MeCN. CF_3SO_3Me (0.08 mL, 0.70 mmol) was added to a MeCN solution (20 mL) of $[Et_4N]_2[Te\{Cr(CO)_5\}_2]$ (0.20 g, 0.26 mmol) in an ice−water bath. The green solution became reddish-orange instantly. After being stirred for 30 min, the solution was filtered, and the solvent was evaporated under vacuum. The residue was washed with hexanes and extracted with ether/THF (v/v 6:1) to yield a yellowish-orange sample of $Me_2Te\{Cr(CO)_5\}_2$ (**2**) (0.12 g, 0.22 mmol) (85% based on $[Et_4N]_2[Te\{Cr(CO)_5\}_2]$). IR ($\nu_{CO}$, ether): 2077 vw, 2060 w, 1960 s, 1940 m cm^{-1}. Mass (EI): calcd (found), 543.8 (543.9). Anal. Calcd for **2**: C, 26.60; H, 1.12. Found: C, 26.88; H, 1.17. ^1H NMR (400 MHz, $CDCl_3$, 300 K, ppm): δ 2.45 (s, CH_3). ^{13}C NMR (100 MHz, $CDCl_3$, 300 K, ppm): δ −0.82 (CH_3), 211.5, 215.0, 217.6, 220.3 (CrCO). Crystals of **2** suitable for single-crystal X-ray diffraction were grown from hexanes/CH_2Cl_2.

Reaction of $[Et_4N][MeTe\{Cr(CO)_5\}_2]$ with CF_3SO_3Me (~1:1.1) in MeCN. CF_3SO_3Me (0.11 mL, 0.97 mmol) was added to a MeCN solution (30 mL) of $[Et_4N][MeTe\{Cr(CO)_5\}_2]$ (0.57 g, 0.87 mmol) at −40 °C. The yellowish-orange solution became reddish-orange instantly. After being stirred for 1 h, the solution was filtered, and the solvent was evaporated under vacuum. The residue was washed with hexanes and extracted with ether/THF (v/v 6:1) to yield a yellowish-orange sample of $Me_2Te\{Cr(CO)_5\}_2$ (**2**) (0.29 g, 0.54 mmol) (62% based on $[Et_4N][MeTe\{Cr(CO)_5\}_2]$).

Reaction of $[Me_4N]_2[Te\{Cr(CO)_5\}_3]$ with CF_3SO_3Me (~1:0.8) in MeCN. CF_3SO_3Me (0.10 mL, 0.87 mmol) was added to a MeCN solution (20 mL) of $[Me_4N]_2[Te\{Cr(CO)_5\}_3]$ (0.90 g, 1.06 mmol) in an ice−water bath. The olive green solution became yellowish-orange instantly. After being stirred for 1 h, the solution was filtered, and the solvent was evaporated under vacuum. The residue was washed several times with hexanes/Et_2O and extracted with THF to yield a reddish-orange sample of $[Me_4N][MeTe\{Cr(CO)_5\}_3]$ ($[Me_4N]$[**3**]) (0.62 g, 0.78 mmol) (90% based on CF_3SO_3Me). IR (ν_{CO}, THF): 2066 w, 2043 m, 2029 w, 1972 w, 1949 vs, 1943 vs, 1921 w, 1901 s cm^{-1}. Anal. Calcd for $[Me_4N]$[**3**]:C, 30.30; H, 1.91; N, 1.77. Found: C, 30.41; H, 1.56; N, 2.05. ^1H NMR (400 MHz, DMSO-d_6, 300 K, ppm): δ 2.07 (s, CH_3) (chemical shifts not given for $[Me_4N]^+$). ^{13}C NMR (100 MHz, DMSO-d_6, 300 K, ppm): δ −15.92 (CH_3), 218.36, 224.41 (CrCO) (chemical shifts not given for $[Me_4N]^+$). Crystals of $[Me_4N]$[**3**] suitable for single-crystal X-ray diffraction were grown from hexanes/Et_2O/THF.

Reaction of $[Et_4N]_2[Te\{Cr(CO)_5\}_2]$ with CH_2Cl_2 (at 0 °C). CH_2Cl_2 (20 mL) was added to a sample of $[Et_4N]_2[Te\{Cr(CO)_5\}_2]$ (0.55 g, 0.71 mmol) in an ice−water bath. The resulting solution was stirred at 0 °C for 2.5 h to produce a yellowish-orange solution. The solution was filtered, and the solvent was evaporated under vacuum. The residue was washed several times with Et_2O and extracted with THF to yield a sample of $[Et_4N][ClH_2CTe\{Cr(CO)_5\}_2]$ ($[Et_4N]$[**4**]) (0.42 g, 0.61 mmol) (86% based on $[Et_4N]_2[Te\{Cr(CO)_5\}_2]$). IR ($\nu_{CO}$, CH_2Cl_2): 2053 w, 2033 s, 1965 w, 1931 vs, 1909 w, 1889 m cm^{-1}. Anal. Calcd for $[Et_4N]$[**4**]: C, 33.01; H, 3.21; N, 2.03. Found: C, 32.80; H, 3.32; N, 1.99. ^1H NMR (400 MHz, DMSO-d_6, 300 K, ppm): δ 4.56 (s, CH_2) (chemical shifts not given for $[Et_4N]^+$). ^{13}C NMR (100 MHz, DMSO-d_6, 300 K, ppm): δ −5.37 (CH_2), 219.9, 226.5 (CrCO) (chemical shifts not given for $[Et_4N]^+$). Crystals of $[Et_4N]$[**4**] suitable for single-crystal X-ray diffraction were grown from hexanes/Et_2O/THF.

Reaction of $[Et_4N]_2[Te\{Cr(CO)_5\}_3]$ with CH_2Cl_2 (at 0 °C). CH_2Cl_2 (20 mL) was added to a sample of $[Et_4N]_2[Te\{Cr(CO)_5\}_3]$ (0.38 g, 0.39 mmol) in an ice−water bath. The resulting solution was stirred for 3 h to produce a yellowish-orange solution. The solution was filtered, and the solvent was evaporated under vacuum. The residue was washed several times with Et_2O and extracted with THF to yield a sample of $[Et_4N][ClCH_2Te\{Cr(CO)_5\}_3]$ ($[Et_4N]$[**5**]) (0.29 g, 0.33 mmol) (85% based on $[Et_4N]_2[Te\{Cr(CO)_5\}_3]$). IR ($\nu_{CO}$, CH_2Cl_2): 2068 w, 2002 m, 2047 s, 1951 vs, 1901 m cm^{-1}. $[PPN][ClCH_2Te\{Cr(CO)_5\}_3]$ ($[PPN]$[**5**]) was synthesized by a

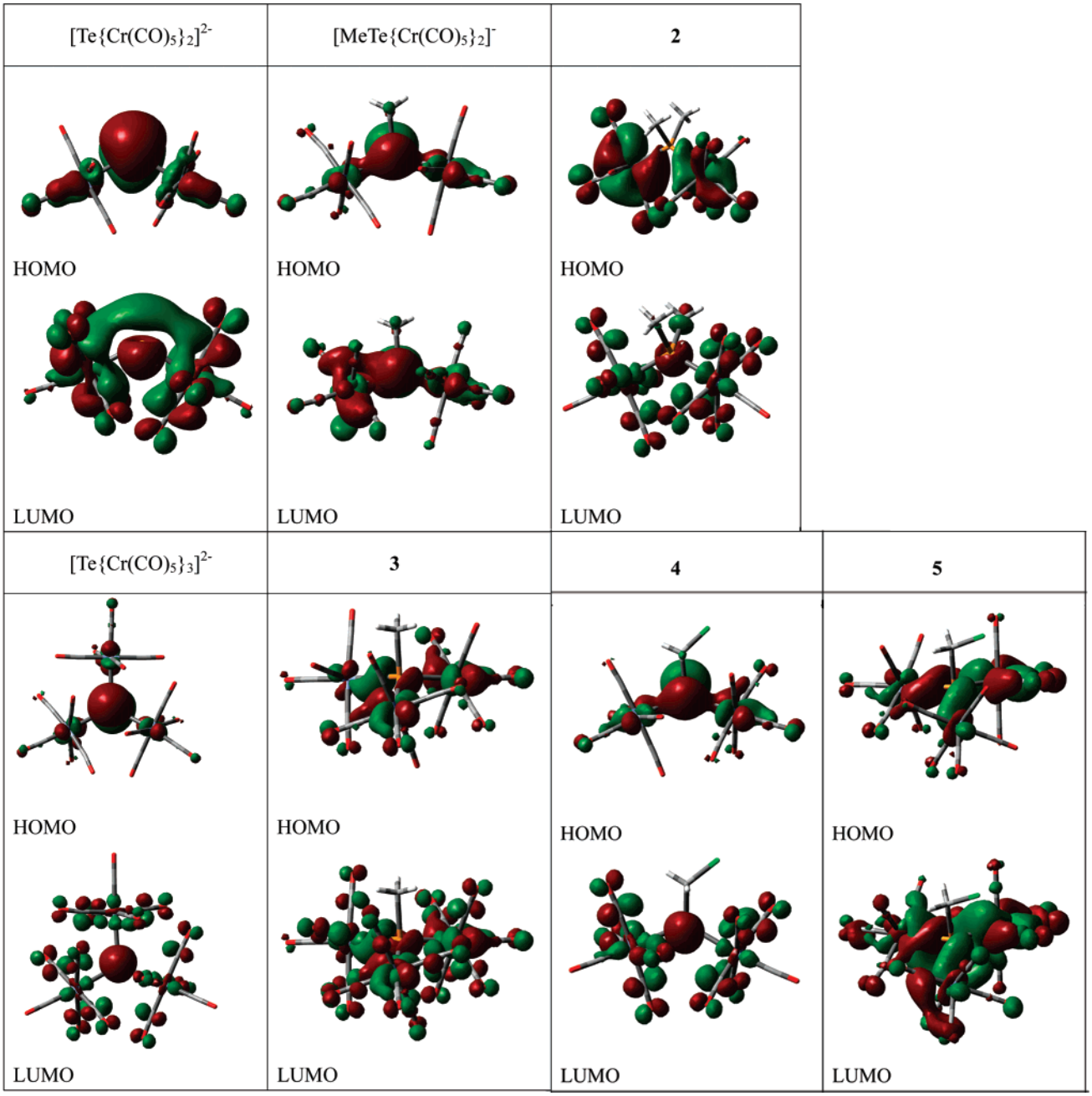

Figure 10. The spatial graphs (isovalue = 0.02−0.04) of the selected frontier molecular orbitals of $[Te\{Cr(CO)_5\}_n]^{2-}$ (n = 2, 3) and related products.

similar procedure using $[PPN]_2[Te\{Cr(CO)_5\}_3]$ as the starting material. Crystals of [PPN][**5**] suitable for single-crystal X-ray diffraction were grown from $MeOH/CH_2Cl_2$. Anal. Calcd for [PPN][**5**]: C, 48.35; H, 2.50; N, 1.08. Found: C, 48.38; H, 2.62; N, 0.82. ^{1}H NMR (400 MHz, DMSO-d_6, 300 K, ppm): δ 4.55 (s, CH_2) (chemical shifts not given for $[PPN]^+$). ^{13}C NMR (100 MHz, DMSO-d_6, 300 K, ppm): δ −6.41 (CH_2), 215.4, 221.6, 228.3 (CrCO) (chemical shifts not given for $[PPN]^+$).

Reaction of $[Et_4N]_2[Te\{Cr(CO)_5\}_3]$ with CH_2Cl_2 (at rt). CH_2Cl_2 (40 mL) was added to a sample of $[Et_4N]_2[Te\{Cr(CO)_5\}_3]$ (0.77 g, 0.80 mmol) at room temperature. The resulting solution was stirred at room temperature for 20 h to produce a yellowish-orange solution. The solution was filtered, and the solvent was evaporated under vacuum. The residue was washed several times with Et_2O and extracted with THF to yield a sample of $[Et_4N]_2[H_2CTe_2\{Cr(CO)_5\}_6]$ ($[Et_4N]_2$[**6**]) (0.39 g, 0.23 mmol) (58% based on $[Et_4N]_2[Te\{Cr(CO)_5\}_3]$). IR ($\nu_{CO}$, CH_2Cl_2): 2045 m, 2034 m, 1933 vs, 1880 s cm^{-1}. Anal. Calcd for $[Et_4N]_2$[**6**]: C, 33.56; H, 2.52; N, 1.67. Found: C, 33.70; H, 2.58; N, 1.68. ^{1}H NMR (400 MHz, DMSO-d_6, 300 K, ppm): δ 4.55 (s, CH_2) (chemical shifts not given for $[Et_4N]^+$). ^{13}C NMR (100 MHz, DMSO-d_6, 300 K, ppm): δ −5.45 (CH_2), 213.6, 217.2, 220.5, 223.7, 227.6 (CrCO) (chemical shifts not given for $[Et_4N]^+$). Crystals of $[Et_4N]_2$[**6**] suitable for single-crystal X-ray diffraction were grown from hexanes/Et_2O/THF.

Reaction of $[Et_4N][ClH_2CTe\{Cr(CO)_5\}_2]$ ($[Et_4N]$[4]) with $[Et_4N]_2[Te\{Cr(CO)_5\}_2]$ in MeCN. $[Et_4N]_2[Te\{Cr(CO)_5\}_2]$ (0.24 g, 0.31 mmol) was added to a MeCN solution (20 mL) of $[Et_4N]$[**4**] (0.21 g, 0.30 mmol) at ambient temperature. The resulting solution was stirred for 30 min to produce an orange-brown solution. The solution was filtered, and the solvent was evaporated under vacuum. The residue was washed several times with Et_2O and extracted with THF to yield a reddish-orange sample of $[Et_4N]_2[H_2CTe_2\{Cr(CO)_5\}_4]$[10a] (0.24 g, 0.18 mmol) (58% based on $[Et_4N]_2[Te\{Cr(CO)_5\}_2]$). IR ($\nu_{CO}$, THF): 2052 m, 2034 m, 1932 vs, 1887 s cm^{-1}.

Table 3. Natural Bond Order and Natural Population Analyses of $[Te\{Cr(CO)_5\}_2]^{2-}$, $[MeTe\{Cr(CO)_5\}_2]^-$, 2, $[Te\{Cr(CO)_5\}_3]^{2-}$, and 3

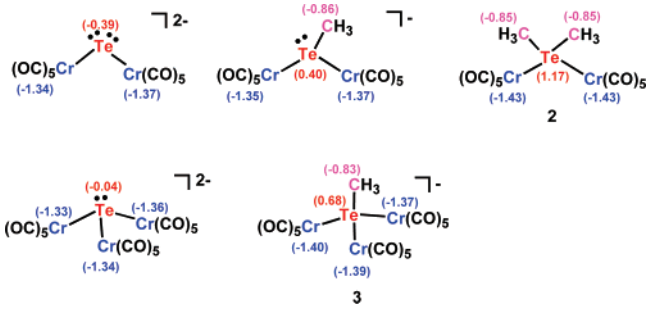

complex	Wiberg bond index Te−Cr	Wiberg bond index Te−C	natural charge Te	natural charge Cr	natural charge C
$[Te\{Cr(CO)_5\}_2]^{2-}$	0.35		−0.39	−1.36	
$[MeTe\{Cr(CO)_5\}_2]^-$	0.36	0.93	+0.40	−1.36	−0.86
2	0.37	0.91	+1.17	−1.43	−0.85
$[Te\{Cr(CO)_5\}_3]^{2-}$	0.35[a]		−0.04	−1.34	
	0.34[b]				
3	0.35[a]	0.92	0.68	−1.39	−0.83
	0.35[b]				

[a] Calculated at the level of B3LYP/LANL2DZ. [b] Calculated at the level of MP2/ LANL2DZ.

Table 4. Results of Natural Bond Order and Natural Population Analyses of the Te−X−Te Complexes 9, 10, 11, and $[H_2CTe_2\{Cr(CO)_5\}_4]^{2-}$ (X = Hg, O, and CH_2)

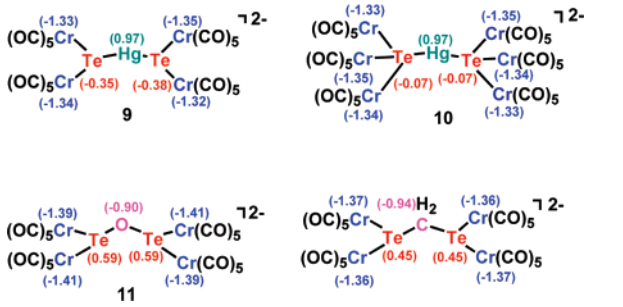

complex	Wiberg bond index Te−Cr	Wiberg bond index Te−X	natural charge Te	natural charge Cr	natural charge X
9 (X = Hg)	0.35	0.50	−0.37	−1.34	+0.97
10 (X = Hg)	0.33	0.46	−0.07	−1.34	+0.97
11 (X = O)	0.40	0.72	+0.59	−1.40	−0.90
$[H_2CTe_2\{Cr(CO)_5\}_4]^{2-}$ (X = CH_2)	0.37	0.90	+0.45	−1.37	−0.94

[a] Calculated at the level of B3LYP/LANL2DZ. [b] Calculated at the level of MP2/LANL2DZ.

Reaction of $[Me_4N][ClCH_2Te\{Cr(CO)_5\}_3]$ ($[Me_4N][5]$) with $[Me_4N]_2[Te\{Cr(CO)_5\}_3]$ in MeCN. $[Me_4N]_2[Te\{Cr(CO)_5\}_3]$ (0.28 g, 0.33 mmol) was added to a MeCN solution (20 mL) of $[Me_4N]$-[**5**] (0.27 g, 0.33 mmol) at ambient temperature. The resulting solution was stirred for 26 h to produce a reddish-orange solution. The solution was filtered, and the solvent was evaporated under vacuum. The residue was washed several times with Et_2O and extracted with THF to yield a reddish-orange sample of $[Me_4N]_2[H_2$-$CTe_2\{Cr(CO)_5\}_6]$ ($[Me_4N]_2$[**6**]) (0.32 g, 0.20 mmol) (61% based on $[Me_4N]$[**5**]). IR (ν_{CO}, THF): 2045 w, 2034 w, 1932 vs, 1880 s cm^{-1}.

Reaction of $[Et_4N]_2[Te\{Cr(CO)_5\}_2]$ with $ClH_2C(C_6H_4)_2CH_2Cl$ in Acetone. $ClH_2C(C_6H_4)_2CH_2Cl$ (0.14 g, 0.56 mmol) was added to an acetone solution (20 mL) of $[Et_4N]_2[Te\{Cr(CO)_5\}_2]$ (0.88 g, 1.14 mmol) in an ice−water bath. The green solution became orange instantly. After being stirred for 30 min, the solution was filtered, and the solvent was evaporated under vacuum. The residue was washed several times with hexanes/Et_2O and extracted with THF to yield a yellowish-orange sample of $[Et_4N]_2[H_2C(C_6H_4)_2CH_2Te_2$-$\{Cr(CO)_5\}_4]$ ($[Et_4N]_2$[**7**]) (0.67 g, 0.46 mmol) (81% based on $[Et_4N]_2[Te\{Cr(CO)_5\}_2]$). IR ($\nu_{CO}$, THF): 2049 w, 2029 m, 1962 m, 1962 w, 1926 vs, 1905 m, 1887 s cm^{-1}. Anal. Calcd for $[Et_4N]_2$-[**7**]: C, 41.02; H, 3.58; N, 1.91. Found: C, 40.74; H, 3.64; N, 1.93. ^1H NMR (400 MHz, DMSO-d_6, 300 K, ppm): δ 3.97 (s, CH_2), δ 7.30, 7.32, 7.49, 7.51 (m, C_6H_4) (chemical shifts not given for $[Et_4N]^+$). ^{13}C NMR (100 MHz, DMSO-d_6, 300 K, ppm): δ −1.28 (CH_2), 126.5, 130.2, 137.4, 142.6 (C_6H_4), 219.6, 220.3, 226.5 (CrCO) (chemical shifts not given for $[Et_4N]^+$). Crystals of $[Et_4N]_2$-[**7**] suitable for single-crystal X-ray diffraction were grown from Et_2O/MeCN.

Reaction of $[Me_4N]_2[Te\{Cr(CO)_5\}_3]$ with $ClH_2C(C_6H_4)_2CH_2Cl$ in THF. $ClH_2C(C_6H_4)_2CH_2Cl$ (0.21 g, 0.84 mmol) was added to a THF solution (30 mL) of $[Me_4N]_2[Te\{Cr(CO)_5\}_3]$ (1.48 g, 1.74 mmol) in an ice−water bath. The olive green solution became yellowish-brown instantly. After being stirred for 60 min, the solution was filtered, and the solvent was evaporated under vacuum. The residue was washed several times with hexanes/Et_2O and extracted with THF to yield a yellow sample of $[Me_4N]_2[H_2C$-$(C_6H_4)_2CH_2Te_2\{Cr(CO)_5\}_6]$ ($[Me_4N]_2$[**8**]) (0.31 g, 0.18 mmol) (21% based on $ClH_2C(C_6H_4)_2CH_2Cl$). IR (ν_{CO}, THF): 2065 w, 2043 s, 1975 w, 1944 vs, 1900 vs cm^{-1}. Anal. Calcd for $[Me_4N]_2$[**8**]: C, 35.98; H, 2.09; N, 1.61. Found: C, 37.42; H, 2.78; N, 1.58. ^1H NMR (400 MHz, DMSO-d_6, 300 K, ppm): δ 3.98 (s, CH_2), δ 7.49, 7.32 (m, C_6H_4) (chemical shifts not given for $[Et_4N]^+$). ^{13}C NMR (100 MHz, DMSO-d_6, 300 K, ppm): δ −0.98 (CH_2), 126.6, 129.0, 137.8, 143.0 (C_6H_4), 213.6, 218.3, 220.6, 225.9 (CrCO) (chemical shifts not given for $[Me_4N]^+$). Crystals of $[Me_4N]_2$[**8**] suitable for single-crystal X-ray diffraction were grown from hexanes/Et_2O/THF.

Reaction of $[Et_4N]_2[Te\{Cr(CO)_5\}_2]$ with $HgCl_2$ in MeCN. $HgCl_2$ (0.09 g, 0.33 mmol) was added to a MeCN solution (20 mL) of $[Et_4N]_2[Te\{Cr(CO)_5\}_2]$ (0.41 g, 0.53 mmol) in an ice−water bath. The green solution became orange instantly and was then stirred for 30 min to produce an orange-brown solution. The solution was filtered, and the solvent was evaporated under vacuum. The residue was washed several times with Et_2O and extracted with THF to yield a reddish-orange sample of $[Et_4N]_2[HgTe_2\{Cr(CO)_5\}_4]$ ($[Et_4N]_2$[**9**]) (0.31 g, 0.21 mmol) (79% based on $[Et_4N]_2[Te\{Cr$-$(CO)_5\}_2]$). IR (ν_{CO}, THF): 2044 s, 2032 s, 1938 vs, 1922 m, 1878 s cm^{-1}. Anal. Calcd for $[Et_4N]_2$[**9**]: C, 29.00; H, 2.71; N, 1.88. Found: C, 29.13; H, 2.52; N, 2.05. Crystals of $[Et_4N]_2$[**9**] suitable for single-crystal X-ray diffraction were grown from Et_2O/MeOH/THF.

Reaction of $[Et_4N]_2[Te\{Cr(CO)_5\}_3]$ with $HgCl_2$ in THF. $HgCl_2$ (0.17 g, 0.63 mmol) was added to a THF solution (30 mL) of $[Et_4N]_2[Te\{Cr(CO)_5\}_3]$ (1.24 g, 1.29 mmol) in an ice−water bath. The olive green solution became reddish-orange instantly and was then stirred for 30 min to yield a red solution. The solution was

Table 5. Calculated Percentage Contribution Ratios of the Te, Cr, Hg, O, and C Atoms to Selected Frontier Molecular Orbitals of the Te−X−Te Complexes (X = Hg, O, and CH_2)

species	atoms Te	atoms Cr	atoms X
9 (HOMO)	24% p	19% d	2% d
9 (LUMO)	29% s + 19% p	1% p	23% s + 1% p
10 (HOMO)	12% p	32% d	3% p
10 (LUMO)	34% s + 12% p	2% d	30% s
11 (HOMO)	4% s + 24% p	4% p + 12% d	10% p
11 (LUMO)	2% s + 38% p	6% p + 2% d	2% s + 14% p
$[H_2CTe_2\{Cr(CO)_5\}_4]^{2-}$ (HOMO)	26% p	16% d	1% p
$[H_2CTe_2\{Cr(CO)_5\}_4]^{2-}$ (LUMO)	24% s + 6% p	14% p + 2% d	

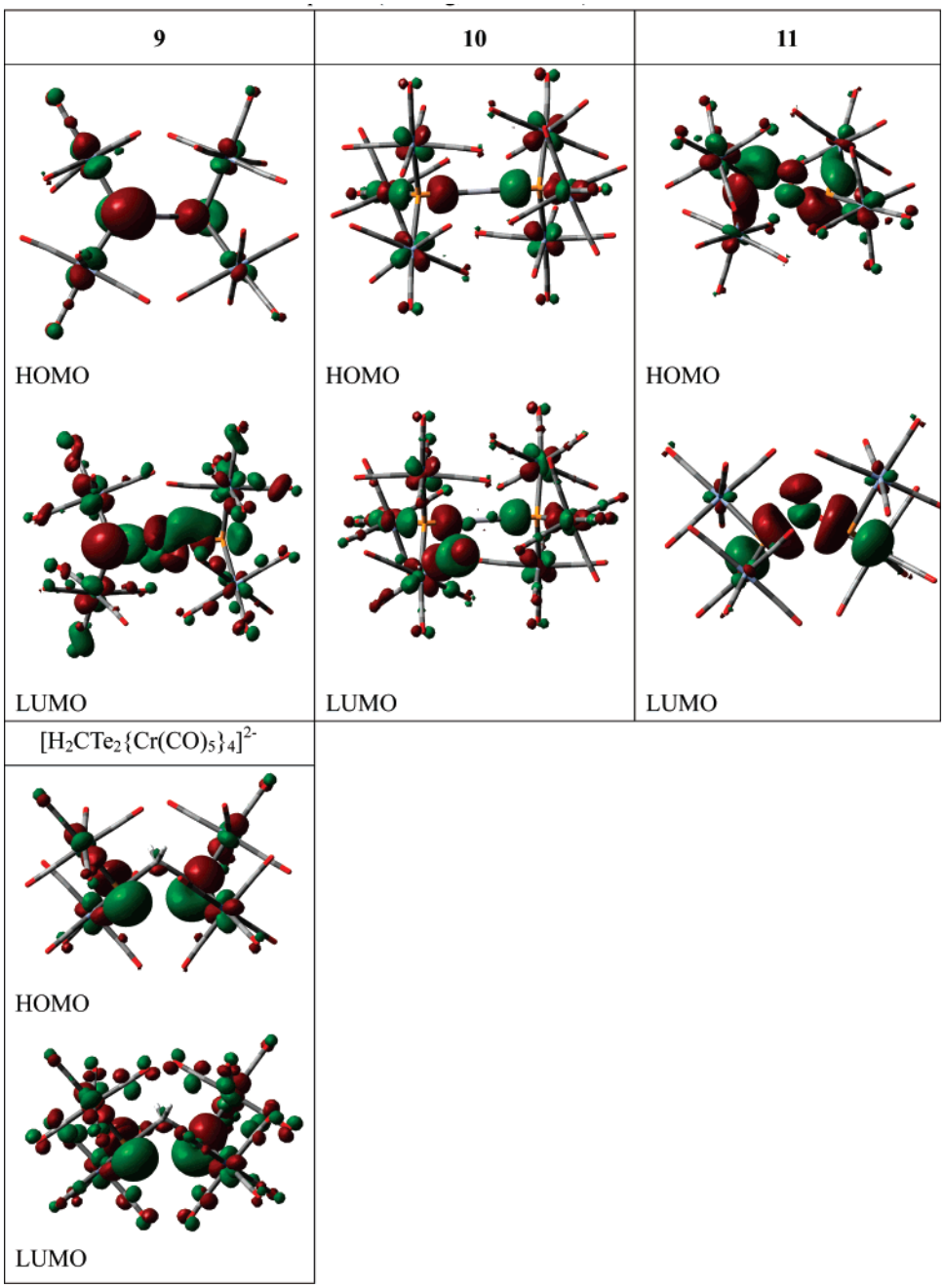

Figure 11. The spatial graphs (isovalue = 0.02−0.04) of the selected frontier molecular orbitals of the Te−X−Te complexes (X = Hg, O, and CH_2).

filtered, and the solvent was evaporated under vacuum. The residue was washed several times with Et_2O and extracted with THF to produce a red sample of $[Et_4N]_2[HgTe_2\{Cr(CO)_5\}_6]$ ($[Et_4N]_2$[**10**]) (0.51 g, 0.27 mmol) (43% based on $HgCl_2$). IR (ν_{CO}, THF): 2057 s, 2032 s, 1980 w, 1946 vs, 1938 vs, 1895 s cm^{-1}. Anal. Calcd for $[Et_4N]_2$[**10**]: C, 29.57; H, 2.16; N, 1.50. Found: C, 29.66; H, 2.32; N, 1.69. Crystals of $[Et_4N]_2$[**10**] suitable for single-crystal X-ray diffraction were grown from Et_2O/MeOH/THF.

Reaction of $[Et_4N]_2[HgTe_2\{Cr(CO)_5\}_4]$ ($[Et_4N]_2$[9]) with $HgCl_2$ in THF. $HgCl_2$ (0.03 g, 0.11 mmol) was added to a THF solution (25 mL) of $[Et_4N]_2$[**9**] (0.40 g, 0.27 mmol) in an ice−water bath. The orange solution became reddish-orange instantly and was then stirred for 30 min to produce a red solution. The solution was filtered, and the solvent was evaporated under vacuum. The residue was washed several times with Et_2O and extracted with THF to yield a red sample of $[Et_4N]_2[HgTe_2\{Cr(CO)_5\}_6]$ ($[Et_4N]_2$[**10**]) (0.10 g, 0.05 mmol) (19% based on $[Et_4N]_2$[**9**]).

Reaction of $[Et_4N]_2[Te\{Cr(CO)_5\}_2]$ with O_2 in MeCN. Oxygen gas was bubbled through a MeCN solution (25 mL) of $[Et_4N]_2[Te\{Cr(CO)_5\}_2]$ (0.34 g, 0.44 mmol) in an ice−water bath. The green solution became reddish-brown instantly. After being stirred for 1 h, the solution was filtered, and the solvent was evaporated under vacuum. The residue was washed several times with Et_2O and extracted with CH_2Cl_2 to produce a reddish-brown sample of $[Et_4N]_2[OTe_2\{Cr(CO)_5\}_4]$ ($[Et_4N]_2$[**11**]) (0.27 g, 0.21 mmol) (95% based on $[Et_4N]_2[Te\{Cr(CO)_5\}_2]$). IR ($\nu_{CO}$, THF): 2045 m, 2034 m, 1933 vs, 1882 s cm^{-1}. Anal. Calcd for $[Et_4N]_2$[**11**]: C, 33.26; H, 3.10; N, 2.16. Found: C, 32.87; H, 3.48; N, 2.42. Crystals of $[Et_4N]_2$[**11**] suitable for single-crystal X-ray diffraction were grown from hexanes/CH_2Cl_2.

Reaction of $[Et_4N]_2[Te\{Cr(CO)_5\}_3]$ with O_2 in THF. Oxygen gas was bubbled through a THF solution (20 mL) of $[Et_4N]_2[Te\{Cr(CO)_5\}_3]$ (0.61 g, 0.63 mmol) at −40 °C. The olive green solution became yellow-brown instantly. After being stirred for 30

Table 6. Crystallographic Data for 2, $[Me_4N][3]$, $[Et_4N][4]$, and [PPN][5]

	2	$[Me_4N]$[**3**]	$[Et_4N]$[**4**]	[PPN][**5**]
empirical formula	$C_{12}H_6Cr_2O_{10}Te$	$C_{20}H_{15}Cr_3NO_{15}Te$	$C_{19}H_{22}ClCr_2NO_{10}Te$	$C_{52}H_{32}ClCr_3NO_{15}P_2Te$
fw	541.77	792.93	691.43	1291.81
cryst syst	monoclinic	triclinic	monoclinic	monoclinic
space group	$P2_1/n$	$P\bar{1}$	$P2_1/n$	$P2_1/c$
crystal dimens, mm	0.18 × 0.15 × 0.09	0.40 × 0.20 × 0.15	0.20 × 0.06 × 0.05	0.30 × 0.25 × 0.20
a, Å	10.4279(2)	8.892(8)	9.282802(2)	14.989(1)
b, Å	12.1706(3)	12.670(5)	13.3823(1)	20.001(2)
c, Å	14.0655(4)	13.25(1)	22.5814(5)	18.590(2)
α, deg		90.90(5)		
β, deg	99.893(1)	90.66(7)	100.218(1)	98.42(1)
γ, deg		91.76(6)		
V, Å^3	1758.56(7)	1492(2)	2759.7(1)	5513(1)
Z	4	2	4	4
D(calcd), g cm^{-3}	2.046	1.765	1.664	1.520
μ, mm^{-1}	2.908	2.097	1.968	1.270
diffractometer	Nonius (Kappa CCD)	Nonius (CAD4)	Nonius (Kappa CCD)	Nonius (CAD4)
radiation (*λ*), Å	0.71073	0.71073	0.71073	0.71073
temp, K	200(2)	293(2)	293(2)	293(2)
θ range for data collecn, deg	2.23−25.69	1.53−24.92	2.26−25.06	1.50−24.92
T_{min}/T_{max}	0.56/0.79	0.54/0.72	0.78/0.87	0.71/0.74
no. of indep reflns ($I > 2\sigma(I)$)	2752 ($R_{int} = 0.0767$)	4059 ($R_{int} = 0.0267$)	2757 ($R_{int} = 0.0748$)	6591 ($R_{int} = 0.0279$)
R1[a]/wR2[a] ($I > 2\sigma(I)$)	0.039/0.102	0.053/0.146	0.058/0.154	0.039/0.117
R1[a]/wR2[a] (all data)	0.054/0.129	0.073/0.157	0.116/0.183	0.077/0.136

[a] The functions minimized during least-squares cycles were $R1 = \sum||F_o| - |F_c||/\sum|F_o|$ and $wR2 = [\sum[w(F_o^2 - F_c^2)^2]/\sum[w(F_o^2)^2]]^{1/2}$.

Table 7. Crystallographic Data for $[Et_4N]_2$[7], $[Me_4N]_2$[8], $[Et_4N]_2$[9], $[Et_4N]_2$[10], and $[Et_4N]_2$[11]

	$[Et_4N]_2$[**7**]	$[Me_4N]_2$[**8**]	$[Et_4N]_2$[**9**]	$[Et_4N]_2$[**10**]	$[Et_4N]_2$[**11**]
empirical formula	$C_{58}H_{68}Cr_4N_2O_{22}Te_2$	$C_{60}H_{52}Cr_6N_2O_{32}Te_2$	$C_{36}H_{40}Cr_4HgN_2O_{20}Te_2$	$C_{46}H_{40}Cr_6HgN_2O_{30}Te_2$	$C_{36}H_{40}Cr_4N_2O_{21}Te_2$
fw	1608.34	1880.24	1484.49	1868.59	1299.90
cryst syst	monoclinic	monoclinic	monoclinic	triclinic	orthorhombic
space group	$P2_1/n$	$P2_1/n$	$P2_1/c$	$P\bar{1}$	*Fddd*
crystal dimens, mm	0.80 × 0.60 × 0.44	0.20 × 0.11 × 0.07	0.21 × 0.16 × 0.12	0.16 × 0.09 × 0.03	0.30 × 0.25 × 0.10
a, Å	9.357(3)	9.8092(1)	15.2744(2)	10.2579(2)	11.744(3)
b, Å	36.21(1)	18.6258(2)	11.0433(2)	12.6000(2)	35.263(6)
c, Å	10.548(3)	41.9228(5)	30.4798(6)	12.9949(3)	51.38(1)
α, deg				89.3168(7)	
β, deg	94.136(5)	94.850(7)	93.7891(6)	72.3148(7)	
γ, deg				85.5263(1)	
V, Å^3	3564(2)	7632.1(2)	5129.9(2)	1595.24(5)	21 276(8)
Z	2	4	4	1	16
D(calcd), g cm^{-3}	1.499	1.636	1.922	1.945	1.623
μ, mm^{-1}	1.465	1.656	4.988	4.361	1.940
diffractometer	Siemens (SMART CCD)	Nonius (Kappa CCD)	Nonius (Kappa CCD)	Nonius (Kappa CCD)	Nonius (CAD4)
radiation (*λ*), Å	0.71073	0.71073	0.71073	0.71073	0.71073
temp, K	293(2)	200(2)	200(2)	200(2)	293(2)
θ range for data collecn, deg	2.01−25.00	2.08−25.96	1.83−25.06	2.09−25.03	1.58−24.91
T_{min}/T_{max}	0.77/0.96	0.74/0.87	0.40/0.46	0.61/0.73	0.71/0.82
no. of indep reflns ($I > 2\sigma(I)$)	5917 ($R_{int} = 0.0470$)	8398 ($R_{int} = 0.0999$)	6612 ($R_{int} = 0.0574$)	4465 ($R_{int} = 0.0702$)	2707 ($R_{int} = 0.0000$)
R1[a]/wR2[a] ($I > 2\sigma(I)$)	0.085/0.211	0.056/0.140	0.046/0.109	0.044/0.103	0.035/0.085
R1[a]/wR2[a] (all data)	0.089/0.214	0.118/0.191	0.073/0.135	0.066/0.135	0.102/0.105

[a] The functions minimized during least-squares cycles were $R1 = \sum||F_o| - |F_c||/\sum|F_o|$ and $wR2 = [\sum[w(F_o^2 - F_c^2)^2]/\sum[w(F_o^2)^2]]^{1/2}$.

min, the solution was filtered, and the solvent was evaporated under vacuum. The residue was washed several times with Et_2O and extracted with THF to produce a sample of $[Et_4N]_2[Te_2\{Cr(CO)_5\}_4]$ (0.11 g, 0.09 mmol) (29% based on $[Et_4N]_2[Te\{Cr(CO)_5\}_3]$), which was further confirmed by X-ray analysis. IR (ν_{CO}, THF): 2058 w, 2038 m, 2031 s, 1965 w, 1929 vs, 1907 w, 1873 s cm^{-1}.

X-ray Structural Characterization of 2, $[Me_4N][3]$, $[Et_4N][4]$, [PPN][5], $[Et_4N]_2$[7], $[Me_4N]_2$[8], $[Et_4N]_2$[9], $[Et_4N]_2$[10], and $[Et_4N]_2$[11]. Selected crystallographic data for **2**, $[Me_4N]$[**3**], $[Et_4N]$[**4**], [PPN][**5**], $[Et_4N]_2$[**7**], $[Me_4N]_2$[**8**], $[Et_4N]_2$[**9**], $[Et_4N]_2$[**10**], and $[Et_4N]_2$[**11**] are shown in Tables 6 and 7. Selected distances and angles for **2**, $[Me_4N]$[**3**], $[Et_4N]$[**4**], [PPN][**5**], $[Et_4N]_2$[**7**], $[Me_4N]_2$[**8**], $[Et_4N]_2$[**9**], $[Et_4N]_2$[**10**], and $[Et_4N]_2$[**11**] are shown in Table 8. Data collection for **2**, $[Et_4N]$[**4**], $[Me_4N]_2$[**8**], $[Et_4N]_2$[**9**], and $[Et_4N]_2$[**10**] was conducted using a Brucker-Nonius Kappa CCD diffractometer with graphite-monochromated Mo Kα radiation at 298 K.

Table 8. Selected Bond Distances (Å) and Bond Angles (deg) for 2, [Me_4N][3], [Et_4N][4], [PPN][5], [Et_4N]$_2$[7], [Me_4N]$_2$[8], [Et_4N]$_2$[9], [Et_4N]$_2$[10], and [Et_4N]$_2$[11]

		2	
Te(1)−C(11)	2.135(7)	C(11)−Te(1)−C(12)	93.2(3)
Te(1)−C(12)	2.135(5)	C(11)−Te(1)−Cr(1)	110.3(2)
Te(1)−Cr(1)	2.6400(9)	C(12)−Te(1)−Cr(1)	105.7(2)
Te(1)−Cr(2)	2.6468(9)	C(11)−Te(1)−Cr(2)	112.4(2)
		C(12)−Te(1)−Cr(2)	108.7(2)
		Cr(1)−Te(1)−Cr(2)	122.36(3)
		[Me_4N][**3**]	
Te(1)−C(16)	2.154(7)	C(16)−Te(1)−Cr(1)	100.2(2)
Te(1)−Cr(1)	2.717(2)	C(16)−Te(1)−Cr(2)	103.2(2)
Te(1)−Cr(2)	2.723(3)	Cr(1)−Te(1)−Cr(2)	118.41(6)
Te(1)−Cr(3)	2.734(2)	C(16)−Te(1)−Cr(3)	102.3(2)
		Cr(1)−Te(1)−Cr(3)	114.37(6)
		Cr(2)−Te(1)−Cr(3)	114.80(6)
		[Et_4N][**4**]	
Te(1)−C(11)	2.140(8)	C(11)−Te(1)−Cr(2)	98.9(2)
Te(1)−Cr(2)	2.713(1)	C(11)−Te(1)−Cr(1)	103.6(2)
Te(1)−Cr(1)	2.726(1)	Cr(1)−Te(1)−Cr(2)	118.27(4)
		[PPN][**5**]	
Te(1)−C(16)	2.181(5)	C(16)−Te(1)−Cr(2)	105.4(2)
Te(1)−Cr(2)	2.7097(9)	C(16)−Te(1)−Cr(1)	104.2(2)
Te(1)−Cr(1)	2.7164(9)	Cr(2)−Te(1)−Cr(1)	117.25(3)
Te(1)−Cr(3)	2.7329(8)	C(16)−Te(1)−Cr(3)	97.0(1)
		Cr(2)−Te(1)−Cr(3)	112.13(3)
		Cr(1)−Te(1)−Cr(3)	117.39(3)
		[Et_4N]$_2$[**7**]	
Te(1)−C(11)	2.17(1)	C(11)−Te(1)−Cr(1)	100.8 (3)
Te(1)−Cr(1)	2.724(2)	C(11)−Te(1)−Cr(2)	106.5(3)
Te(1)−Cr(2)	2.727(2)	Cr(1)−Te(1)−Cr(2)	114.19(6)
		[Me_4N]$_2$[**8**]	
Te(1)−C(31)	2.226(7)	C(31)−Te(1)−Cr(3)	106.9(2)
Te(1)−Cr(3)	2.726(1)	C(31)−Te(1)−Cr(2)	106.2(2)
Te(1)−Cr(2)	2.734(1)	Cr(3)−Te(1)−Cr(2)	113.12(4)
Te(1)−Cr(1)	2.756(1)	C(31)−Te(1)−Cr(1)	98.2(2)
Te(2)−C(44)	2.214(8)	Cr(3)−Te(1)−Cr(1)	113.26(4)
Te(2)−Cr(6)	2.734(1)	Cr(2)−Te(1)−Cr(1)	117.17(4)
Te(2)−Cr(5)	2.738(1)	C(44)−Te(2)−Cr(6)	110.1(2)
Te(2)−Cr(4)	2.744(1)	C(44)−Te(2)−Cr(5)	99.2(2)
		Cr(6)−Te(2)−Cr(5)	113.17(4)
		C(44)−Te(2)−Cr(4)	106.40(2)
		Cr(6)−Te(2)−Cr(4)	114.30(4)
		Cr(5)−Te(2)−Cr(4)	112.36(4)
		[Et_4N]$_2$[**9**]	
Hg(1)−Te(1)	2.6395(6)	Te(1)−Hg(1)−Te(2)	173.79(2)
Hg(1)−Te(2)	2.6398(6)	Hg(1)−Te(1)−Cr(2)	98.56(3)
Te(1)−Cr(2)	2.751(1)	Hg(1)−Te(1)−Cr(1)	98.75(3)
Te(1)−Cr(1)	2.781(1)	Cr(2)−Te(1)−Cr(1)	115.67(4)
Te(2)−Cr(4)	2.726(1)	Hg(1)−Te(2)−Cr(4)	103.83(3)
Te(2)−Cr(3)	2.745(1)	Hg(1)−Te(2)−Cr(3)	105.64(3)
		Cr(4)−Te(2)−Cr(3)	116.92(4)
		[Et_4N]$_2$[**10**]	
Hg(1)−Te(1)	2.6955(4)	Te(1)−Hg(1)−Te(1a)	180.00(2)
Cr(1)−Te(1)	2.731(1)	Hg(1)−Te(1)−Cr(3)	106.39(3)
Cr(2)−Te(1)	2.741(1)	Hg(1)−Te(1)−Cr(1)	104.06(3)
Cr(3)−Te(1)	2.725(1)	Cr(3)−Te(1)−Cr(1)	112.87(4)
		Hg(1)−Te(1)−Cr(2)	98.87(3)
		Cr(3)−Te(1)−Cr(2)	114.90(4)
		Cr(1)−Te(1)−Cr(2)	117.35(4)
		[Et_4N]$_2$[**11**]	
O(11)−Te(1a)	2.252(5)	Te(1a)−O(11)−Te(1)	108.2(3)
O(11)−Te(1)	2.252(5)	O(11)−Te(1)−Cr(2)	94.8(2)
Cr(1)−Te(1)	2.746(1)	O(11)−Te(1)−Cr(1)	106.11(5)
Cr(2)−Te(1)	2.728(1)	Cr(3)−Te(1)−Cr(1)	112.88(3)

An empirical absorption correction by multiscans was applied. Data collection for [Me_4N][**3**], [PPN][**5**], and [Et_4N]$_2$[**11**] was conducted using a Nonius (CAD-4) diffractometer with graphite-monochromated Mo Kα radiation at 293 K in the 2θ range of 2.0−50°. An empirical absorption correction by azimuthal (ψ) scans was applied.[21] Data collection for [Et_4N]$_2$[**7**] was conducted using a Siemens SMART CCD (charged coupled device) diffractometer. The structures were solved by direct methods and were refined by SHELXL packages.[22] All of the non-hydrogen atoms for **2**, [Me_4N]-[**3**], [Et_4N][**4**], [PPN][**5**], [Et_4N]$_2$[**7**], [Me_4N]$_2$[**8**], [Et_4N]$_2$[**9**], [Et_4N]$_2$-[**10**], and [Et_4N]$_2$[**11**] were refined with anisotropic temperature factors. Additional crystallographic data in the form of CIF files are available as Supporting Information.

Computational Details. All calculations reported in this study were performed via the density functional theory (DFT) with Becke's three-parameter (B3) exchange functional and the Lee−Yang−Parr (LYP) correlation functional (B3LYP)[16,17] or the second-order Møller−Plesset (MP2)[23] method with a LanL2DZ basis set using the Gaussian 03 series of packages.[24] The geometries of all of the calculated complexes were taken from the crystal structures without further modification. Wiberg bond indices[18] and natural charges[19] were evaluated using the Weinhold NBO method.[25] Graphic representations of the molecular orbitals were obtained using Gaussview 3.0.

Acknowledgment. This work was supported by National Science Council of Taiwan (NSC 95-2113-M-003-009-MY3 to M.S.). We are also grateful to the National Center for High-Performance Computing, where the Gaussian package and computer time were provided. Our gratitude also goes to the Academic Paper Editing Clinic, NTNU.

Supporting Information Available: X-ray crystallographic files in CIF format for **2**, [Me_4N][**3**], [Et_4N][**4**], [PPN][**5**], [Et_4N]$_2$[**7**], [Me_4N]$_2$[**8**], [Et_4N]$_2$[**9**], [Et_4N]$_2$[**10**], and [Et_4N]$_2$[**11**]. Computational details for complexes [$Te\{Cr(CO)_5\}_n]^{2-}$ ($n=2,3$), [$MeTe\{Cr(CO)_5\}_2]^-$, **2**, **3**, **4**, **5**, **9**, **10**, **11**, and [$H_2CTe_2\{Cr(CO)_5\}_4]^{2-}$. This material is available free of charge via the Internet at http://pubs.acs.org.

OM700789A

(21) North, A. C. T.; Philips, D. C.; Mathews, F. S. *Acta Crystallogr.* **1968**, *A24*, 351.

(22) Sheldrick, G. M. *SHELXL97*, version 97-2; University of Göttingen: Germany, 1997.

(23) Møller, C.; Plesset, M. S. *Phys. Rev.* **1934**, *46*, 618.

(24) Frisch, M. J.; Trucks, G. W.; Schlegel, H. B.; Scuseria, G. E.; Robb, M. A.; Cheeseman, J. R.; Montgomery, J. A., Jr.; Vreven, T.; Kudin, K. N.; Burant, J. C.; Millam, J. M.; Iyengar, S. S.; Tomasi, J.; Barone, V.; Mennucci, B.; Cossi, M.; Scalmani, G.; Rega, N.; Petersson, G. A.; Nakatsuji, H.; Hada, M.; Ehara, M.; Toyota, K.; Fukuda, R.; Hasegawa, J.; Ishida, M.; Nakajima, T.; Honda, Y.; Kitao, O.; Nakai, H.; Klene, M.; Li, X.; Knox, J. E.; Hratchian, H. P.; Cross, J. B.; Bakken, V.; Adamo, C.; Jaramillo, J.; Gomperts, R.; Stratmann, R. E.; Yazyev, O.; Austin, A. J.; Cammi, R.; Pomelli, C.; Ochterski, J. W.; Ayala, P. Y.; Morokuma, K.; Voth, G. A.; Salvador, P.; Dannenberg, J. J.; Zakrzewski, V. G.; Dapprich, S.; Daniels, A. D.; Strain, M. C.; Farkas, O.; Malick, D. K.; Rabuck, A. D.; Raghavachari, K.; Foresman, J. B.; Ortiz, J. V.; Cui, Q.; Baboul, A. G.; Clifford, S.; Cioslowski, J.; Stefanov, B. B.; Liu, G.; Liashenko, A.; Piskorz, P.; Komaromi, I.; Martin, R. L.; Fox, D. J.; Keith, T.; Al-Laham, M. A.; Peng, C. Y.; Nanayakkara, A.; Challacombe, M.; Gill, P. M. W.; Johnson, B.; Chen, W.; Wong, M. W.; Gonzalez, C.; Pople, J. A. *Gaussian 03*, revision B.04; Gaussian, Inc.: Wallingford, CT, 2004.

(25) Reed, A. E.; Curtiss, L. A.; Weinhold, F. *Chem. Rev.* **1988**, *88*, 899.